

Model Uncertainty in Performance Assessment for the Proposed Yucca Mountain Repository for High-Level Radioactive Waste

J.C. Helton^a, C.W. Hansen^b, C.J. Sallaberry^b

^aDepartment of Mathematics and Statistics, Arizona State University, Tempe, AZ 85287-1804

^bSandia National Laboratories, Albuquerque, NM 87185-1370

Abstract

The appropriate treatment of model uncertainty is an important and difficult challenge in the analysis of complex systems. The conceptual treatment of model uncertainty is complicated by the fact that parameter uncertainty grades into model uncertainty with no clear boundary between where parameter uncertainty ends and model uncertainty begins. The intent of this presentation is to solve neither the challenge of how to unambiguously define model uncertainty nor the general challenge of how to appropriately incorporate representations for model uncertainty into an analysis. Rather, the intent is to provide perspectives on both the indicated challenges by providing examples of how model uncertainty was defined and incorporated into the 2008 performance assessment for the proposed geologic repository for high-level radioactive waste under development by the U.S. Department of Energy at Yucca Mountain, Nevada. Specifically, five examples of the incorporation of model uncertainty into the 2008 Yucca Mountain performance assessment are presented: uncertain model for infiltration and unsaturated flow properties, uncertain model for CO₂ partial pressure in waste disposal drifts, uncertain model for plutonium solubility, uncertain model for a Poisson process, and uncertain model for dose conversion.

Keywords: Aleatory uncertainty, Epistemic uncertainty, High-level radioactive waste, Model uncertainty, Performance assessment, Sensitivity analysis, Uncertainty analysis, Yucca Mountain

1. Introduction

As is now widely recognized, the appropriate representation of uncertainty is an important part of any analysis [1-8]. Further, the uncertainties that must be considered in the analysis of a complex system are often subdivided into two classes: aleatory uncertainty and epistemic uncertainty [9-15]. Specifically, aleatory uncertainty corresponds to the uncertainty that derives from randomness in the properties or the behavior of the system under study (e.g., the magnitude and time of occurrence of a future seismic event), and epistemic uncertainty corresponds to the uncertainty that derives from a lack of knowledge with respect to the appropriate value to use for a quantity that is assumed to have a fixed value in the context of a specific analysis (e.g., the appropriate value to use for a spatially-averaged permeability). In turn, epistemic uncertainties are often divided into parameter uncertainty and model uncertainty, where parameter uncertainty corresponds to epistemic uncertainty in the appropriate value to use for a quantity that is an input to a model and model uncertainty corresponds to epistemic uncertainty with respect to the appropriate model to use to represent a physical process or some other aspect of the behavior of a system. Parameter uncertainty and its effects on model predictions has long been an area of study [16-25]. Model uncertainty has been less studied than parameter uncertainty but is an area in which interest is rapidly increasing [26-34].

The conceptual treatment of model uncertainty is complicated by the fact that parameter uncertainty grades into model uncertainty with no clear boundary between where parameter

uncertainty ends and model uncertainty begins. The intent of this presentation is to solve neither the challenge of how to unambiguously define model uncertainty nor the challenge of how to appropriately incorporate representations for model uncertainty into an analysis. Rather, the intent is to provide perspectives on both the indicated challenges by providing five examples of the treatment of model uncertainty in the 2008 performance assessment (PA) for the proposed geologic repository for high-level radioactive waste under development by the U.S. Department of Energy at Yucca Mountain (YM), Nevada [35-40].

The presentation is organized as follows. First, a brief overview of the 2008 YM PA is given (Sect. 2). Next, the five examples of the incorporation of model uncertainty into the 2008 YM PA are presented: uncertain model for infiltration and unsaturated flow properties (Sect. 3), uncertain model for CO₂ partial pressure in waste disposal drifts (Sect. 4), uncertain model for plutonium solubility (Sect. 5), uncertain model for a Poisson process (Sect. 6), and uncertain model for dose conversion (Sect. 7). The presentation then ends with a concluding discussion (Sect. 8).

2. Overview of the 2008 Yucca Mountain Performance Assessment

This section is written to provide an overview of the 2008 PA for the proposed YM repository for high-level radioactive waste and is adapted from Sect. III of Ref. [41]. Additional and more detailed information on this analysis is contained in Ref. [40] and in the many specialized reports cited in this reference. In particular, the conceptual structure and computational organization of the 2008 YM PA are described in App. J of Ref. [40].

The NRC's requirements for the YM repository [42-44] in 10 CFR Part 63 result in a PA that involves three basic entities: EN1, a characterization of the uncertainty in the occurrence of future events (e.g., igneous events, seismic events) that could affect the performance of the repository; EN2, models for predicting the physical behavior and evolution of the repository (e.g., systems of ordinary and partial differential equations); and EN3, a characterization of the uncertainty associated with analysis inputs that have fixed but imprecisely known values (e.g., the appropriate value to use for a dose conversion factor) [45; 46]. The designators aleatory and epistemic are commonly used for the uncertainties characterized by entities EN1 and EN3 [9; 11-15].

In the preceding, aleatory uncertainty is used in the designation of, in so far as our ability to predict the future is concerned, randomness in the possible future conditions that could affect the YM repository. In concept, each possible future at the YM repository can be represented by a vector

$$\mathbf{a} = [a_1, a_2, \dots, a_{nA}], \tag{2.1}$$

where each a_i is a specific property of the future \mathbf{a} (e.g., time of a seismic event, size of a seismic event, ...) and the random events characterized by the individual futures occur in a specified time interval $[a, b]$ (e.g., $[0, 20,000 \text{ yr}]$ or $[0, 1,000,000 \text{ yr}]$ in the 2008 YM PA). In turn, a subset Σ of the set A of all possible values for \mathbf{a} constitutes what is referred to as a scenario class in the

2008 YM PA. As part of the 2008 YM PA development, a probabilistic structure is imposed on the set A . Formally, this corresponds to defining a probability space (A, \mathcal{A}, p_A) for aleatory uncertainty. As a reminder with respect to the properties of an arbitrary probability space (A, \mathcal{A}, p_A) , the set A contains everything that could occur in the particular “universe” under consideration; \mathcal{A} is a suitably restricted set of subsets of A for which probability is defined; and p_A is a function that defines the probability of individual elements of A (see Ref. [47], Sect. IV.3, for additional discussion of probability spaces). In the context of the 2008 YM PA, A is the set of all possible scenario classes, and p_A is the function that defines scenario class probability (i.e., scenario class Σ is an element of A and $p_A(\Sigma)$ is the probability of scenario class Σ). Formally, the probability space (A, \mathcal{A}, p_A) provides a characterization of aleatory uncertainty and constitutes the first of the three basic mathematical entities that underlie the determination of expected dose to the reasonably maximally exposed individual (RMEI) specified in 10 CFR Part 63 and, in addition, many other results relevant to the performance of the YM repository.

Although useful conceptually and notationally, the probability space (A, \mathcal{A}, p_A) is never explicitly defined in the 2008 YM PA. Rather, the characterization of aleatory uncertainty enters the analysis through the definition of probability distributions for the individual elements of \mathbf{a} . Conceptually, the distributions for the elements of \mathbf{a} lead to a distribution for \mathbf{a} and an associated density function $d_A(\mathbf{a})$. The nature of the probability space (A, \mathcal{A}, p_A) in the context of the 2008 YM PA for events taking place over a specified time interval $[a, b]$ is indicated in Table 1 (see Ref. [40], App. J, for additional information). Different, but closely related, probability spaces result for $[a, b] = 20,000$ yr and $[a, b] = 1,000,000$ yr and underlie different parts of the 2008 YM PA.

Table 1 Aleatory Uncertainty in the 2008 YM PA ([41], Table I)

<p>Individual Futures (i.e., elements of sample space A):</p> $\mathbf{a} = [n_{EW}, n_{ED}, n_{II}, n_{IE}, n_{SG}, n_{SF}, \mathbf{a}_{EW}, \mathbf{a}_{ED}, \mathbf{a}_{II}, \mathbf{a}_{IE}, \mathbf{a}_{SG}, \mathbf{a}_{SF}]$ <p>where, for a specified time interval $[a, b]$, n_{EW} = number of early waste package (WP) failures, n_{ED} = number of</p>
--

early drip shield (DS) failures, nII = number of igneous intrusive events, nIE = number of igneous eruptive events, nSG = number of seismic ground motion (GM) events, nSF = number of seismic fault displacement (FD) events, \mathbf{a}_{EW} = vector defining the nEW early WP failures, \mathbf{a}_{ED} = vector defining the nED early DS failures, \mathbf{a}_{II} = vector defining the nII igneous intrusive events, \mathbf{a}_{IE} = vector defining the nIE igneous eruptive events, \mathbf{a}_{SG} = vector defining the nSG seismic GM events, and \mathbf{a}_{SF} = vector defining the nSF seismic FD events.

Sample Space for Aleatory Uncertainty:

$$A = \{ \mathbf{a} : \mathbf{a} = [nEW, nED, nII, nIE, nSG, nSF, \mathbf{a}_{EW}, \mathbf{a}_{ED}, \mathbf{a}_{II}, \mathbf{a}_{IE}, \mathbf{a}_{SG}, \mathbf{a}_{SF}] \}$$

High-Level Scenario Classes (i.e., Elements of set A):

Nominal, $A_N = \{ \mathbf{a} : \mathbf{a} \in A \text{ and } nEW = nED = nII = nIE = nSG = nSF = 0 \}$

Early WP failure, $A_{EW} = \{ \mathbf{a} : \mathbf{a} \in A \text{ and } nEW \geq 1 \}$

Early DS failure, $A_{ED} = \{ \mathbf{a} : \mathbf{a} \in A \text{ and } nED \geq 1 \}$

Igneous intrusive, $A_{II} = \{ \mathbf{a} : \mathbf{a} \in A \text{ and } nII \geq 1 \}$

Igneous eruptive, $A_{IE} = \{ \mathbf{a} : \mathbf{a} \in A \text{ and } nIE \geq 1 \}$

Seismic GM, $A_{SG} = \{ \mathbf{a} : \mathbf{a} \in A \text{ and } nSG \geq 1 \}$

Seismic FD, $A_{SF} = \{ \mathbf{a} : \mathbf{a} \in A \text{ and } nSF \geq 1 \}$

Scenario Class Probabilities:

$p_A(A_N)$ = probability of no disruptions of any kind

$p_A(A_{EW})$ = probability of one or more early WP failures

$p_A(A_{ED})$ = probability of one or more early DS failures

$p_A(A_{II})$ = probability of one or more igneous intrusive events

$p_A(A_{IE})$ = probability of one or more igneous eruptive events

$p_A(A_{SG})$ = probability of one or more seismic GM events

$p_A(A_{SF})$ = probability of one or more seismic FD events

The second of the three basic mathematical entities that underlie the 2008 YM PA is a model that predicts dose to the RMEI and many additional results. Formally, this model can be represented by the function

$$D(\tau | \mathbf{a}) = \text{dose to RMEI (mrem/yr) at time } \tau \text{ (yr) conditional on the occurrence of } \quad (2.2)$$

the future represented by \mathbf{a} .

Technically, $D(\tau | \mathbf{a})$ is the committed 50 yr dose to the RMEI that results from radiation exposure incurred in a single year. Model uncertainty is present with respect to the appropriate choice of models to represent and calculate $D(\tau | \mathbf{a})$; examples of the uncertainty associated with such choices are the subject of this presentation. In the computational implementation of the 2008 YM PA, $D(\tau | \mathbf{a})$ corresponds to the calculation performed for the particular analysis configuration defined for the future \mathbf{a} . In practice, many results are calculated for \mathbf{a} in addition

to dose to the RMEI (e.g., see Ref. [40], Table K3-4); several of these results are used as examples in Sects. 3–7. Thus, $D(\tau|\mathbf{a})$ is actually a vector $\mathbf{D}(\tau|\mathbf{a})$ containing at least several thousand elements. The general nature of $\mathbf{D}(\tau|\mathbf{a})$ is described in Ref. [40] and in the many specialized references cited in Ref. [40]. With respect to terminology, $\mathbf{D}(\tau|\mathbf{a})$ is typically referred to as the Total System Performance Assessment-License Application (TSPA-LA) model in Ref. [40], and, similarly, the 2008 YM PA is referred to as the TSPA-LA analysis. As an example, the overall structure of the model involved in the determination of $\mathbf{D}(\tau|\mathbf{a})$ for the igneous intrusive scenario class is shown in Fig. 1. In general, a variety of analysis results is associated with each of the individual models indicated in Fig. 1.

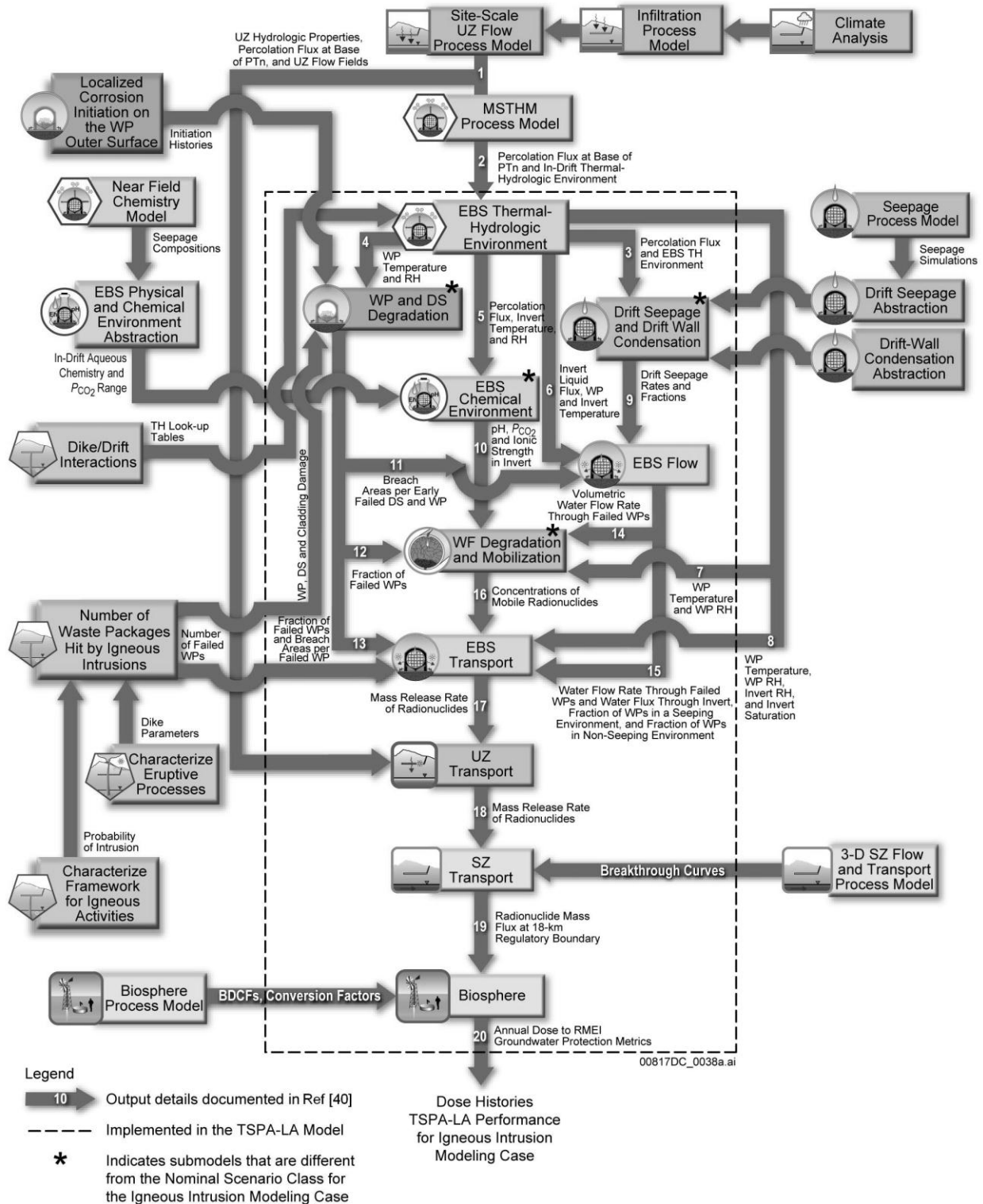


Fig. 1 Information transfer between model components and submodels for the igneous intrusive scenario class in the 2008 YM PA ([40], Fig. 6.1.4-4).

The third of the three basic mathematical entities that underlie the 2008 YM PA is a probabilistic characterization of epistemic uncertainty. Here, epistemic uncertainty refers to a lack of knowledge with respect to the appropriate value to use for a quantity that is assumed to have a constant or fixed value in the context of a specific analysis. Specifically, epistemic uncertainty relates to a vector of the form

$$\begin{aligned} \mathbf{e} &= [\mathbf{e}_A, \mathbf{e}_M] \\ &= [e_{A1}, e_{A2}, \dots, e_{A,nAE}, e_{M1}, e_{M2}, \dots, e_{M,nME}] \\ &= [e_1, e_2, \dots, e_{nE}], nE = nAE + nME, \end{aligned} \quad (2.3)$$

where

$$\mathbf{e}_A = [e_{A1}, e_{A2}, \dots, e_{A,nAE}]$$

is a vector of epistemically uncertain quantities used in the characterization of aleatory uncertainty (e.g., a rate term that defines a Poisson process) and

$$\mathbf{e}_M = [e_{M1}, e_{M2}, \dots, e_{M,nME}]$$

is a vector of epistemically uncertain quantities used in the determination of dose and other analysis results (e.g., a distribution coefficient). Further, the individual elements of \mathbf{e} are interpreted broadly enough to include designators for alternative models or model structures. As a result, model uncertainty formally enters into the 2008 YM PA through the specification of elements of \mathbf{e} and the uncertainty associated with these elements.

Epistemic uncertainty results in a set E of possible values for \mathbf{e} . In turn, probability is used to characterize the level of likelihood or credence that can be assigned to various subsets of E . In concept, this leads to a probability space (E, \mathcal{E}, p_E) for epistemic uncertainty. Like the probability space (A, \mathcal{A}, p_A) for aleatory uncertainty, the probability space (E, \mathcal{E}, p_E) for epistemic uncertainty is useful conceptually and notationally but is never explicitly defined in the 2008 YM PA. Rather, the characterization of epistemic uncertainty enters the analysis through the definition of probability distributions for the individual elements of \mathbf{e} . These distributions serve as mathematical summaries of all available information with respect to where the appropriate values for individual elements of \mathbf{e} are located for use in the 2008 YM PA. Conceptually, the distributions for the elements of \mathbf{e} lead to a distribution for \mathbf{e} and an associated density function $d_E(\mathbf{e})$. The nature of the probability space (E, \mathcal{E}, p_E) in the context of the 2008 YM PA is indicated in

Table 2; a full listing of the elements of \mathbf{e} and sources of additional information are provided in Tables K3-1, K3-2 and K3-3 of Ref. [40].

Table 2 Examples of the $nE = 392$ Epistemically Uncertain Variables in the 2008 YM PA ([41], Table I)

<i>ASHDENS</i> - Tephra settled density (kg/m ³). <i>Distribution</i> : Truncated normal. <i>Range</i> : 300 to 1500. <i>Mean</i> : 1000. <i>Standard Deviation</i> : 100.
<i>IGRATE</i> - Frequency of intersection of the repository footprint by a volcanic event (yr ⁻¹). <i>Distribution</i> : Piecewise uniform. <i>Range</i> : 0 to 7.76E-07.
<i>INFIL</i> - Pointer variable for determining infiltration conditions: 10 th , 30 th , 50 th or 90 th percentile infiltration scenario (dimensionless). <i>Distribution</i> : Discrete. <i>Range</i> : 1 to 4.
<i>MICPU239</i> - Groundwater biosphere dose conversion factor (BDCF) for ²³⁹ Pu in modern interglacial climate ((Sv/year)/(Bq/m ³)). <i>Distribution</i> : Discrete. <i>Range</i> : 3.49E-07 to 2.93E-06. <i>Mean</i> : 9.55E-07.
<i>SZFISPVO</i> - Flowing interval spacing in fractured volcanic units (m). <i>Distribution</i> : Piecewise uniform. <i>Range</i> : 1.86 to 80.

With the introduction of the vector \mathbf{e} of epistemically uncertain analysis inputs and the associated probability space (E, E, p_E) , the vector $\mathbf{D}(\tau|\mathbf{a})$ of analysis results is now appropriately represented by $\mathbf{D}(\tau|\mathbf{a}, \mathbf{e})$ to indicate that its value is conditional on the vector \mathbf{e} . Further, the elements of $\mathbf{D}(\tau|\mathbf{a}, \mathbf{e})$ have distributions that derive from the probability space (E, E, p_E) . In the 2008 YM PA, the epistemic uncertainty associated with the elements of $\mathbf{D}(\tau|\mathbf{a}, \mathbf{e})$ is determined with use of a Latin hypercube sample (LHS)

$$\mathbf{e}_i = [\mathbf{e}_{Ai}, \mathbf{e}_{Mi}], i = 1, 2, \dots, nLHS, \quad (2.4)$$

of size $nLHS = 300$ from the possible values for \mathbf{e} generated in consistency with the distributions that define the probability space (E, E, p_E) (see Refs. [48; 49] for details on Latin hypercube sampling). The 2008 YM PA was then carried out for each element of this sample. The results of these calculations are mappings of the form

$$[\mathbf{e}_i, \mathbf{D}(\tau|\mathbf{a}, \mathbf{e}_i)], i = 1, 2, \dots, nLHS = 300, \quad (2.5)$$

between uncertain analysis inputs \mathbf{e}_i and uncertain analysis results $\mathbf{D}(\tau|\mathbf{a}, \mathbf{e}_i)$ for selected futures \mathbf{a} . These mappings then formed the basis for extensive uncertainty and sensitivity analyses carried out as part of the 2008 YM PA (see Apps. J and K of Ref. [40]). Further, a small subset of these analyses is used in the illustration of the treatment of model uncertainty in the following five sections.

3. Uncertain Model for Infiltration and Unsaturated Flow Properties

The appropriate representation of surface infiltration and unsaturated flow properties in the unsaturated zone (UZ) surrounding the excavated component of the YM repository is an important component of the 2008 PA for the YM repository. In general, both surface infiltration and unsaturated flow properties are functions of time t . Further, surface infiltration (units: m³/m²s) is a two-dimensional function $I(x,y,t)$ of surface location in xy space, and unsaturated flow properties are a three-dimensional vector function $\mathbf{u}(x,y,z,t)$ of location in the UZ. Included in the unsaturated flow properties that constitute elements of $\mathbf{u}(x,y,z,t)$ are water flow in fractures, water flow in matrices surrounding fractures, water saturations in fractures and

surrounding matrices, and water flow between fractures and surrounding matrices. In the 2008 YM PA, $\mathbf{u}(x,y,z,t)$ is estimated on the basis of three submodels: a model for climate change [50; 51], a model for infiltration [52], and a model for two-phase unsaturated fluid flow [53]. Specifically, the model for climate change provides input to a surface infiltration model that determines $I(x,y,t)$, and $I(x,y,t)$ is an input to an unsaturated flow model that determines $\mathbf{u}(x,y,z,t)$. In turn, $\mathbf{u}(x,y,z,t)$ is then input to several other models in the 2008 YM PA.

The climate model is simple in the sense that it corresponds to a direct specification of future climate conditions rather than to an algorithmic or equation-based procedure for the calculation of future climate conditions [50; 51]. In particular, present day climate conditions are assumed to hold over the time interval [0, 600 yr] after repository closure; monsoonal climate conditions are assumed to hold over the time interval [600, 2000 yr]; glacial-transition climate conditions are assumed to hold over the time interval [2000, 10,000 yr]; and infiltration-related conditions deriving from climate change are specified by regulation for the time period following 10,000 yr. In addition, climate properties related to precipitation and temperature are specified for the first three time intervals.

The infiltration model is a complex mathematical model that calculates infiltration on the basis of a number of environmental and climate-related conditions (e.g., soil depth, precipitation, vegetative cover, plant rooting depth, bedrock saturated conductivity, ...) [52]. The infiltration model determines the water flow downward across the upper boundary of the region in which two-phase fluid flow is modeled. Thus, in essence, the infiltration model determines the upper boundary conditions for the two-phase fluid flow model.

The two-phase fluid flow model is a system of nonlinear partial differential equations that are numerically solved with finite difference procedures [53]. Processes incorporated into the two-phase fluid flow model include flow in both fractures and porous material, coupling of flow in fractures and porous material, specification of different properties for individual geologic strata, and explicit incorporation of the locations and properties of major faults. Evaluating the two-phase fluid flow model entails significant computational cost.

The 2008 YM PA felt that it was important to incorporate the effects and implications of uncertainty in the combined infiltration and unsaturated flow model. However this had to be done in a way that held computational costs to a reasonable level. This was accomplished by making an assessment of the uncertainty in the function $\mathbf{u}(x,y,z,t)$. Then, $\mathbf{u}(x,y,z,t)$ could be treated as simply one more epistemically uncertain input to the 2008 YM PA.

The uncertainty associated with $\mathbf{u}(x,y,z,t)$ was characterized as follows. First, it was decided to treat $\mathbf{u}(x,y,z,t)$ as being piecewise constant for the time intervals [0, 600 yr], [600, 2000 yr], [2000, 10,000 yr] and [10,000, 1,000,000 yr] obtained from the climate model. Then, the uncertainty in infiltration was assessed for each of the preceding time intervals. For the individual time intervals [0, 600 yr], [600, 2000 yr] and [2000, 10,000 yr], the uncertainty associated with infiltration was initially assessed by (i) developing probability distributions to characterize the epistemic uncertainty in the variables used as inputs to the infiltration model for each time interval, (ii) generating and pooling two LHSs of size 20 from the uncertain variables for each time interval (Note: These LHSs are different from the LHS indicated in Eq. (2.4)), (iii)

calculating an infiltration field for each LHS element (Reminder: infiltration is variable at the surface in xy space), and then (iv) identifying 0.1, 0.3, 0.5 and 0.9 quantile infiltration fields on the basis of spatially-averaged infiltration across each field ([52], Sect. 6.5). This results in four infiltration fields for each of the time intervals [0, 600 yr], [600, 2000 yr], and [2000, 10,000 yr]. For notational convenience, the resultant 12 infiltration fields are represented by $I_q(x,y | [a, b])$ for $q = 0.1, 0.3, 0.5$ and 0.9 and $[a,b] = [0, 600 \text{ yr}], [600, 2000 \text{ yr}]$ and $[2000, 10,000 \text{ yr}]$.

For the [10,000, 1,000,000 yr] time interval, 0.1, 0.3, 0.5 and 0.9 quantile infiltration fields were developed from the 12 infiltration fields $I_q(x,y | [a, b])$ on the basis of NRC regulatory requirements. Specifically, NRC regulations mandated the distribution to be used to characterize the epistemic uncertainty in downward water flow at the location of the waste disposal drifts associated with the YM repository for the [10,000, 1,000,000 yr] time interval. To implement this requirement, the four infiltration fields with the highest spatially-averaged infiltration were selected from the 12 infiltration fields $I_q(x,y | [a, b])$ and denoted $I_1(x,y), I_2(x,y), I_3(x,y), I_4(x,y)$. Further, the infiltration fields $I_i(x,y), i = 1, 2, 3, 4$, are ordered so that the spatially-averaged infiltration associated with infiltration field $I_i(x,y)$ is less than the spatially-averaged infiltration associated with infiltration field $I_{i+1}(x,y)$ for $i = 1, 2, 3$. Then, the infiltration fields $I_i(x,y)$ were linearly scaled to produce new infiltration fields $SI_i(x,y)$ defined by

$$SI_i(x, y) = k_i I_i(x, y) \quad (3.1)$$

for $i = 1, 2, 3, 4$, where the k_i are constants such that the spatially-averaged infiltrations associated with $SI_1(x,y), SI_2(x,y), SI_3(x,y)$ and $SI_4(x,y)$ are equal to the spatially averaged downward water flows at the location of the waste disposal drifts corresponding to the 0.1, 0.3, 0.5 and 0.9 quantiles, respectively, of the NRC specified distribution. Consistent with this scaling, $SI_1(x,y), SI_2(x,y), SI_3(x,y)$ and $SI_4(x,y)$ were taken to be the 0.1, 0.3, 0.5 and 0.9 quantile infiltration fields for the [10,000, 1,000,000 yr] time interval ([53], Sect. 6.1.4). As above, these four infiltration fields are represented by $I_q(x,y | [10,000, 1,000,000 \text{ yr}])$ for $q = 0.1, 0.3, 0.5$ and 0.9 .

The infiltration fields $I_q(x,y | [a,b])$ defined above were then used to define time-dependent infiltration fields for the time interval [0, 1,000,000 yr]. Specifically, the assumption is made that the infiltration fields across time associated with a given quantile value should be combined to obtain the corresponding infiltration field for the time interval [0, 1,000,000 yr]. Logic for this combination procedure is that the same underlying physical and environmental conditions should cause correspondingly low and high infiltration results across the different climate conditions. As a consequence, the infiltration filtration fields for the time interval [0, 1,000,000 yr] are defined by

$$\begin{aligned} I_q(x, y, t) &= I_q(x, y | [0, 600 \text{ yr}]) \text{ for } 0 \leq t \leq 600 \text{ yr} \\ &= I_q(x, y | [600, 2000 \text{ yr}]) \text{ for } 600 < t \leq 2000 \text{ yr} \\ &= I_q(x, y | [2000, 10,000 \text{ yr}]) \text{ for } 2000 < t \leq 10,000 \text{ yr} \\ &= I_q(x, y | [10,000, 1,000,000 \text{ yr}]) \text{ for } 10,000 < t \leq 1,000,000 \text{ yr} \end{aligned} \quad (3.2)$$

for $q = 0.1, 0.3, 0.5$ and 0.9 .

The indicated 16 individual infiltration fields were determined using only information about climate and near surface conditions. However, field data on properties of conditions below the near surface provide additional information on the potential appropriateness of the individual flow fields $I_q(x,y | [0, 600 \text{ yr}])$ developed for the $[0, 600 \text{ yr}]$ time interval. Specifically, chloride and temperature data from the unsaturated zone at YM were used in conjunction with a generalized likelihood uncertainty estimate (GLUE) methodology to determine probabilities for the four flow fields developed for the $[0, 600 \text{ yr}]$ time interval ([53], Sect. 6.8.2). The steps in the GLUE methodology are (i) determine prior probabilities for each infiltration field, (ii) perform UZ flow and transport calculations for each infiltration field and, based on model results and observed temperature and chloride data, determine likelihood values, and (iii) obtain new infiltration field probabilities from the prior probabilities and associated likelihoods ([53], Sect. 6.8.5.1). Specifically, the resultant probabilities characterizing epistemic uncertainty in the appropriateness of the 0.1, 0.3, 0.5 and 0.9 quantile infiltration fields $I_q(x,y | [0, 600 \text{ yr}])$ for the $[0, 600 \text{ yr}]$ time interval are 0.62, 0.16, 0.16 and 0.06, respectively ([40], Table 6.3.1-2). Further, because of the anticipated similarity of physical and environmental effects across climate conditions, the same probabilities are assumed to also characterize the epistemic uncertainty associated with the time-dependent flow fields $I_q(x,y,t)$ defined in Eq. (3.2).

In addition, the four present day infiltration fields $I_q(x,y | [0, 600 \text{ yr}])$ were used for model calibration, and the resultant calibrated parameters were used as input to the unsaturated flow model. Specifically, the calibrated parameters for $I_q(x,y | [0, 600 \text{ yr}])$ were used in unsaturated flow calculations associated with the infiltration fields $I_q(x,y | [0, 600 \text{ yr}])$, $I_q(x,y | [600, 2000 \text{ yr}])$, $I_q(x,y | [2000, 10,000 \text{ yr}])$ and $I_q(x,y | [10,000, 1,000,000 \text{ yr}])$ for $q = 0.1, 0.3, 0.5$ and 0.9 ([53], Sect. 6.2.5 and Table 6.2.6). The four infiltration fields $I_q(x,y | [0, 600 \text{ yr}])$ were calibrated against measured water saturation, water potential, perched water occurrences, and pneumatic data ([53], Sect. 6.2). The calibrated parameters included intrinsic permeabilities of the matrix and fracture systems and van Genuchten α and m parameters for describing the saturation-capillary pressure relationships in the fracture and matrix systems ([53], App. B, Tables B1-B4). For notational convenience, the three dimensional calibrated parameters for each infiltration field $I_q(x,y | [0, 600 \text{ yr}])$ can be represented by a vector \mathbf{x}_q for $q = 0.1, 0.3, 0.5$ and 0.9 .

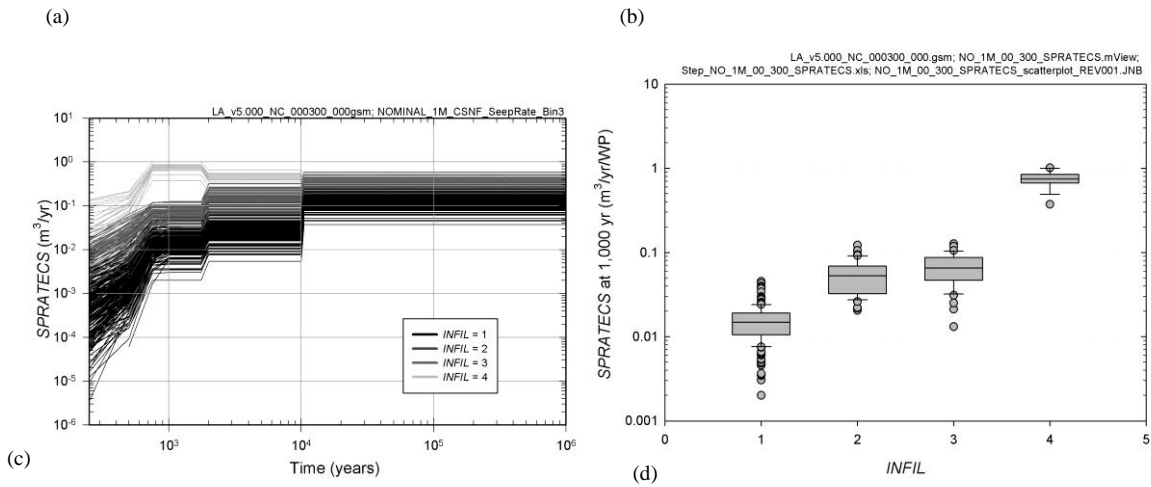
The resultant calibrated parameters \mathbf{x}_q were used as input to the unsaturated flow model. Specifically, the calibrated parameters \mathbf{x}_q for $I_q(x,y | [0, 600 \text{ yr}])$ were used in unsaturated flow calculations associated with the infiltration fields $I_q(x,y | [0, 600 \text{ yr}])$, $I_q(x,y | [600, 2000 \text{ yr}])$, $I_q(x,y | [2000, 10,000 \text{ yr}])$ and $I_q(x,y | [10,000, 1,000,000 \text{ yr}])$ for $q = 0.1, 0.3, 0.5$ and 0.9 ([53], Sect. 6.2.5 and Table 6.2.6). The result of the indicated calculations is a sequence of vectors $\mathbf{u}_q(x,y,z | [0, 600 \text{ yr}])$, $\mathbf{u}_q(x,y,z | [600, 2000 \text{ yr}])$, $\mathbf{u}_q(x,y,z | [2000, 10,000 \text{ yr}])$ and $\mathbf{u}_q(x,y,z | [10,000, 1,000,000 \text{ yr}])$ of UZ properties for $q = 0.1, 0.3, 0.5$ and 0.9 . In the preceding, $\mathbf{u}_q(x,y,z | [0, 600 \text{ yr}])$ is a function of both \mathbf{x}_q and $I_q(x,y | [0, 600 \text{ yr}])$; similar dependencies hold for $\mathbf{u}_q(x,y,z | [600, 2000 \text{ yr}])$, $\mathbf{u}_q(x,y,z | [2000, 10,000 \text{ yr}])$ and $\mathbf{u}_q(x,y,z | [10,000, 1,000,000 \text{ yr}])$.

Time-dependent vectors of UZ properties are now defined by

$$\begin{aligned}
\mathbf{u}_q(x, y, z, t) &= \mathbf{u}_q(x, y, z | [0, 600 \text{ yr}]) \text{ for } 0 \leq t \leq 600 \text{ yr} \\
&= \mathbf{u}_q(x, y, z | [600, 2000 \text{ yr}]) \text{ for } 600 < t \leq 2000 \text{ yr} \\
&= \mathbf{u}_q(x, y, z | [2000, 10,000 \text{ yr}]) \text{ for } 2000 < t \leq 10,000 \text{ yr} \\
&= \mathbf{u}_q(x, y, z | [10,000, 1,000,000 \text{ yr}]) \text{ for } 10,000 < t \leq 1,000,000 \text{ yr}
\end{aligned} \tag{3.3}$$

for $q = 0.1, 0.3, 0.5$ and 0.9 . The vector functions $\mathbf{u}_q(x, y, z, t)$ are treated as epistemically uncertain inputs to the 2008 YM PA with the corresponding probabilities of 0.62, 0.16, 0.16 and 0.06 determined for $I_q(x, y | [0, 600 \text{ yr}])$ and $q = 0.1, 0.3, 0.5$ and 0.9 . In the 2008 YM PA, the uncertain input $\mathbf{u}_q(x, y, z, t)$ is incorporated into the analysis through an epistemically uncertain quantity designated *INFIL* as a mnemonic derived from the role of infiltration in the determination of $\mathbf{u}_q(x, y, z, t)$. Specifically, *INFIL* assumes the possible values of 1, 2, 3 or 4 with probabilities of 0.62, 0.16, 0.16 and 0.06, respectively; in turn, *INFIL* is one of the 392 epistemically uncertain variables sampled in the 2008 YM PA, with *INFIL* = 1 designating the use of $\mathbf{u}_{0.1}(x, y, z, t)$ in PA calculations and analogous designations occurring for *INFIL* = 2, 3 and 4. Additional information and references on the development and use of $\mathbf{u}_q(x, y, z, t)$ in the 2008 YM PA are available in Sect. 6.3.1 of Ref. [40].

The vector functions $\mathbf{u}_q(x, y, z, t)$ play an important role in the 2008 YM PA and are involved in the definition of seepage into the engineered barrier system (EBS) corresponding to the excavated component of the repository system, the determination of thermal and chemical conditions in the EBS, and the representation of radionuclide transport in the UZ beneath the EBS. As single example, the effects of $\mathbf{u}_q(x, y, z, t)$ on seepage into the EBS above a commercial spent nuclear fuel (CSNF) waste package (WP) in percolation bin 3 under nominal conditions are shown in Fig. 2. With respect to terminology, percolation bin 3 is the most extensive of five regions into which the repository footprint is divided for the purpose of calculating seepage into the repository (see [40], Fig. 6.1.4-2), and nominal conditions is a designator for repository conditions that have not been altered by any type of disruptive event (e.g., a seismic event or an igneous event).



SPRATECS: 1,000 yr			
Step	Variable	R ²	SRRC
1	INFIL	0.67	0.83
2	SEEP _{PRM}	0.76	-0.28
3	ALPHAL	0.82	-0.26
4	SEEP _{PRM}	0.85	-0.19
5	SEEP _{UNC}	0.87	0.15
6	INFRCTC	0.88	0.06
7	CORRATSS	0.88	-0.05

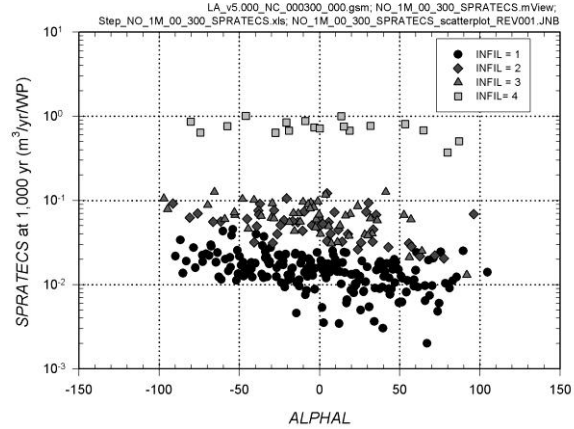


Fig. 2 Seepage rates (*SPRATECS*, m³/yr/WP) above CSNF WPs in percolation bin 3 under nominal conditions obtained with an LHS of size 300: (a) Time-dependent values for *SPRATECS*, (b) Box plots for *SPRATECS* at 1000 yr conditional on individual values for *INFIL*, (c) stepwise rank regression for *SPRATECS* at 1000 yr, and (d) scatterplot for *SPRATECS* at 1000 yr versus *ALPHAL* ([40], Figs. K4.3-1 and K4.3-2).

The time-dependent seepage rates (*SPRATECS*, m³/yr/WP) above individual CSNF WPs in percolation bin 3 are shown in Fig. 2a. Each curve in Fig. 2a was generated with one of the 300 LHS elements used in the propagation of epistemic uncertainty in the 2008 YM PA and was calculated with a specific value for $\mathbf{u}_q(x,y,z,t)$ identified by the sampled pointer variable *INFIL*. Because *SPRATECS* tends to increase with increasing values for surface infiltration, there is an ordering of the curves in Fig. 2a, with lowest curves associated with $\mathbf{u}_{0.1}(x,y,z,t)$, the next highest set of curves associated with $\mathbf{u}_{0.3}(x,y,z,t)$, and similarly increasing values for *SPRATECS* for $\mathbf{u}_{0.5}(x,y,z,t)$ and $\mathbf{u}_{0.9}(x,y,z,t)$. This pattern can be seen in the box plots in Fig. 2b for the values of *SPRATECS* at 1000 yr conditional on individual values for *INFIL*. With respect to notation, the “box” in the indicated box plots extends from the 0.25 quantile to the 0.75 quantile of a distribution; the “bar and whiskers” extend outward to the 0.1 and 0.9 quantiles of the distribution; the solid “dots” represent individual observations outside the 0.1 to 0.9 quantile range of the distribution; and the horizontal line within the box corresponds to the median (i.e., 0.5 quantile) of the distribution. If the individual curves in Fig. 2a were coded with different colors to identify the corresponding sampled value for *INFIL*, the pattern of effects for $\mathbf{u}_q(x,y,z,t)$ shown in the box plots in Fig. 2b would be seen to be consistent through time (see [40], Fig. K4.3-1a). The effects of climate change can also be clearly seen in Fig. 2a as the discontinuities in the individual curves tend to take place at times associated with changes in surface infiltration associated with changes in climate.

The box plots in Fig. 2b conditional on individual values for *INFIL*, and hence on individual values for $\mathbf{u}_q(x,y,z,t)$, constitute one form of sensitivity analysis that shows the importance of $\mathbf{u}_q(x,y,z,t)$ with respect to the epistemic uncertainty associated with possible values for *SPRATECS*. As an example, more formal sensitivity analyses can be performed with procedures based on stepwise rank regression (Fig. 2c). Specifically, the stepwise rank regression in Fig. 2c for *SPRATECS* at 1000 yr shows the variables in the order that they were selected in the stepwise selection process, the cumulative R^2 value with the entry of each variable into the regression model, and the standardized rank regression coefficients (SRRCs) for the individual variables in

the final regression model [24]. As indicated by an R^2 value of 0.67 and a SRRC of 0.83 for *INFIL*, $\mathbf{u}_q(x,y,z,t)$ is the greatest contributor to the uncertainty in *SPRATECS* at 1000 yr.

In addition to *INFIL*, the following variables have lesser effects on the uncertainty in *SPRATECS* at 1000 yr: *SEPPRMN* (mean fracture permeability in nonlithophysal rock units, m^2 ; as sampled, *SEPPRMN* is actually the logarithm of the indicated permeability), *ALPHAL* (capillary strength parameter in lithophysal rock units), *SEPPRM* (mean fracture permeability in lithophysal rock units, m^2 ; as sampled, *SEPPRM* is actually the logarithm of the indicated permeability), and *SEEPUNC* (pointer variable used to determine local seepage rates) (Fig. 2c). The negative effects for *SEPPRMN* and *SEPPRM* result from their role in increasing water flow around the drifts. The negative effect for *ALPHAL* results from increasing the capillary “hold” on water in the drift walls. Finally, increasing *SEEPUNC* tends to increase seepage into the EBS through an upscaling of base seepage rates. Thus, although the uncertainty in $\mathbf{u}_q(x,y,z,t)$ dominates the uncertainty in *SPRATECS* at 1000 yr, several other variables also contribute to this uncertainty. The variables *INFRCTC* (initial release fraction of ^{99}Tc from a CSNF WP) and *CORRATSS* (stainless steel corrosion rate, $\mu\text{m}/\text{yr}$) with no significant effect on the final R^2 value are also selected at the end of the stepwise regression in Fig. 2c. The selection of these two variables is probably spurious as the selection of one or more spurious variables with little effect near the end of a stepwise regression with a large number of candidate variables for inclusion in the regression model is a common occurrence.

The examination of scatterplots is often a useful visual supplement to the results obtained in a stepwise regression analysis. The utility of such plots has already been illustrated by Fig. 2b, which clearly shows the effect of *INFIL*, and hence $\mathbf{u}_q(x,y,z,t)$, on *SPRATECS* at 1000 yr. In addition, the spread in results shown by the individual box plots in Fig. 2b also clearly indicates that other variables in addition to $\mathbf{u}_q(x,y,z,t)$ are affecting the uncertainty in *SPRATECS* at 1000 yr. As another example, the scatterplot in Fig. 2d clearly shows both the dominant positive effect of $\mathbf{u}_q(x,y,z,t)$ on *SPRATECS* at 1000 yr and the lesser negative effect of *ALPHAL* on *SPRATECS* at 1000 yr.

4. Uncertain Model for CO_2 Partial Pressure in Waste Disposal Drifts

The calculation of the partial pressure of CO_2 in the waste disposal drifts of the YM repository after final repository closure (*PCO2*, bars) is difficult because *PCO2* is the result of a number of competing processes, including evaporation, degassing, precipitation, diffusion, advection of gas in fractures, and scavenging of CO_2 by condensation at the cooler ends of the waste disposal drifts. Instead of attempting to incorporate the inherent complexity of a mechanistic model of *PCO2* into the 2008 YM PA, a simpler approach was taken. Specifically, two bounding models for *PCO2* were initially developed ([54], Sect. 6.3.2.8):

- (i) Model 1: Estimates maximum possible CO_2 drift partial pressure $MX\text{CO}_2(t|\mathbf{e}_M)$ at time t conditional on vector \mathbf{e}_M of epistemically uncertain analysis inputs,
- (ii) Model 2: Estimates minimum possible CO_2 drift partial pressure $MN\text{CO}_2(t|\mathbf{e}_M)$ at time t conditional on vector \mathbf{e}_M of epistemically uncertain analysis inputs.

As defined, $MXCO2(t|\mathbf{e}_M)$ and $MNCO2(t|\mathbf{e}_M)$ produce values for $PCO2$ above and below the ambient value of 10^{-3} bars at the elevation of the waste disposal drifts in YM. The value for $PCO2$ defined by $MXCO2(t|\mathbf{e}_M)$ results from regarding the waste disposal drifts as a closed system with the maximum partial pressure for CO_2 determined by the equilibrium between gaseous and aqueous phases of CO_2 at the evaporation front in the host rock. In contrast, $MNCO2(t|\mathbf{e}_M)$ is obtained under the assumption that gas moves freely through fractures in the host rock surrounding the waste disposal drifts with the minimum partial pressure for CO_2 determined from the amount of CO_2 in atmospheric air in the drifts (which may be displaced by water vapor) and the amount of CO_2 released from evaporating water. It was felt that the appropriate value for $PCO2$ should be somewhere between the ambient partial pressure of CO_2 at the elevation of the waste disposal drifts in YM (i.e., 10^{-3} bars) and the bounding values defined by $MXCO2(t|\mathbf{e}_M)$ and $MNCO2(t|\mathbf{e}_M)$. The epistemic uncertainty with respect to the appropriate model to determine $PCO2$ was incorporated into the 2008 YM PA by introducing a variable designated $DELPPCO2$ with a uniform distribution on $[-1, 1]$ that characterized both the uncertainty with respect to whether a model that predicted $PCO2$ to be above 10^{-3} bars or a model that predicted $PCO2$ to be below 10^{-3} bars was appropriate and also the extent to which the model predictions should deviate from 10^{-3} bars. Specifically, a specified value for $DELPPCO2$ defined the corresponding epistemically uncertain value for the function $PCO2(t|\mathbf{e}_M)$ by

$$PCO2(t|\mathbf{e}_M) = \begin{cases} 10^{-3} + DELPPCO2 \left[MXCO2(t|\mathbf{e}_M) - 10^{-3} \right] & \text{if } DELPPCO2 \geq 0 \\ 10^{-3} + |DELPPCO2| \left[MNCO2(t|\mathbf{e}_M) - 10^{-3} \right] & \text{if } DELPPCO2 < 0. \end{cases} \quad (4.1)$$

The preceding specification incorporates (i) a degree of belief probability of 0.5 that the appropriate model to predict $PCO2$ should give a value above 10^{-3} bars, (ii) a degree of belief probability of 0.5 that the appropriate model to predict $PCO2$ should give a value below 10^{-3} bars, (iii) a uniform distribution for $PCO2$ between 10^{-3} bars and $MXCO2(t|\mathbf{e}_M)$ if $PCO2$ should be modeled as being greater than 10^{-3} bars, and (iv) a uniform distribution for $PCO2$ between $MNCO2(t|\mathbf{e}_M)$ and 10^{-3} bars and if $PCO2$ should be modeled as being less than 10^{-3} bars. Additional discussion and references are available in Sects. 6.3.4.2 and 6.3.5.2.3 of Ref. [40].

Similarly to $INFIL$, $DELPPCO2$ was one of the 392 epistemically uncertain analysis inputs sampled in the 2008 YM PA. Each sampled value for $DELPPCO2$ resulted in a different time-dependent model for $PCO2$ as indicated in Eq. (4.1) (Fig. 3). Specifically, the 300 time dependent values for $PCO2(t|\mathbf{e}_M)$ that result from the use of an LHS of size 300 are shown in Fig. 3a. In addition, the scatterplot in Fig. 3b shows the relationship between $PCO2$ and $DELPPCO2$ at 1000 yr. The linear effects of $DELPPCO2$ on $PCO2$ are apparent in this scatterplot. Further, none of the other epistemically uncertain variables affect $PCO2$ for partial pressures less than 10^{-3} bars. However, for partial pressures greater than 10^{-3} bars, it is also apparent that $PCO2$ is affected by additional epistemically uncertain variables that collectively determine the equilibrium between gaseous and aqueous phases of CO_2 at the evaporation front in the host rock. These variables include the composition of seepage water ($SEEPWAT$) and

variables that affect water temperature, i.e., infiltration level (*INFIL*) and thermal conductivity in the host rock surrounding the waste disposal drifts (*THERMCON*) ([54], Sect. 6.15.1).

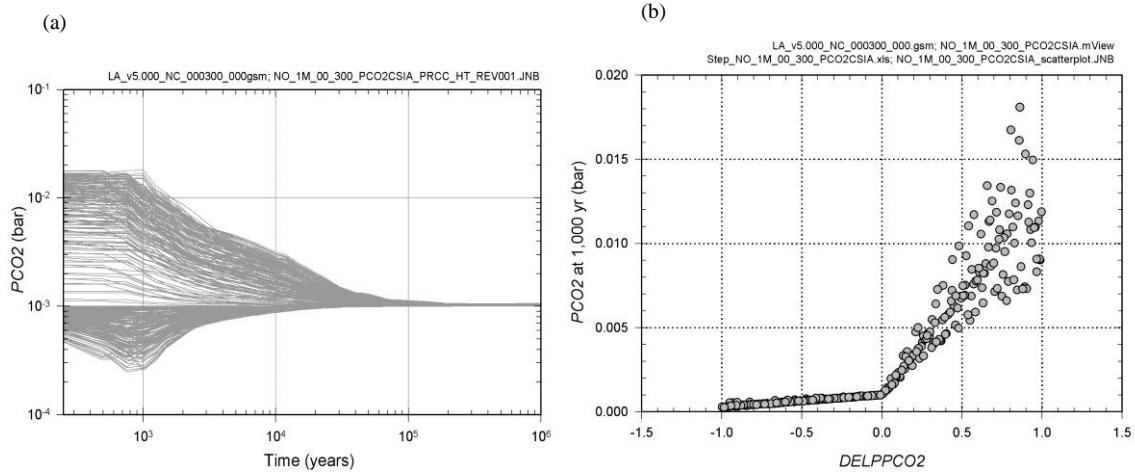


Fig. 3 Partial pressures (PCO_2 , bars) for CO_2 in waste drifts for CSNF WPs experiencing dripping conditions in percolation bin 3 under nominal conditions obtained with an LHS of size 300: (a) Time-dependent values for PCO_2 , and (b) Scatterplot for PCO_2 at 1000 yr versus $DELPPCO_2$ ([40], Figs. K.4.3-7 and K.4.3-7).

5. Uncertain Model for Plutonium Solubility

Plutonium solubility in the EBS in the 2008 YM PA is modeled as function of pH and the fugacity of CO_2 . At the simplest, this results in a model of the form

$$S(t | \mathbf{e}_M) = f [pH(t | \mathbf{e}_M), fCO_2(t | \mathbf{e}_M)], \quad (5.1)$$

where (i) $S(t | \mathbf{e}_M)$ is plutonium solubility (mg/L) at time t , (ii) $pH(t | \mathbf{e}_M)$ is pH at time t , (iii) $fCO_2(t | \mathbf{e}_M)$ is the fugacity of CO_2 at time t , (iv) the values for the preceding quantities are dependent on epistemically uncertain analysis inputs contained in \mathbf{e}_M , and (v) f is an appropriately defined function of $pH(t | \mathbf{e}_M)$ and $fCO_2(t | \mathbf{e}_M)$. However, two potentially important effects were felt to be absent from the preceding model: (i) the potential effects of uncertainties in thermodynamic properties on the definition of the function (i.e., model) f , and (ii) the potential effects of fluoride concentration on plutonium solubility.

To account for the uncertainty resulting from the two missing effects, two uncertain scale factors were incorporated into the solubility model in Eq. (5.1). With this incorporation, the solubility model for plutonium becomes

$$S(t | \mathbf{e}_M) = 10^{\varepsilon_1} f [pH(t | \mathbf{e}_M), fCO_2(t | \mathbf{e}_M)] + \varepsilon_2 N [pH(t | \mathbf{e}_M)], \quad (5.2)$$

where (i) 10^{ε_1} is a scale factor introduced to incorporate the effects of uncertainties in thermodynamic properties into the solubility model, (ii) $N[pH(t|\mathbf{e}_M)]$ is a function that incorporates the effect of fluoride on plutonium solubility as a function of pH, and (iii) ε_2 is a scale factor introduced to incorporate the effects of uncertainties in the definition of $N[pH(t|\mathbf{e}_M)]$ into the solubility model.

The uncertainty terms ε_1 and ε_2 are further refined by specifying uncertainty distributions that are conditional on environmental conditions ([40], Table 6.3.7-44). Specifically, ε_1 is assumed to have a truncated normal distribution on the interval $[-1.4, 1.4]$ with mean 0 and standard deviation 0.7 when ionic strength is less than 1.0 molal and to have a truncated normal distribution on the interval $[-1.52, 1.52]$ with mean 0 and standard deviation 0.76 when ionic strength is between 1.0 molal and 3.0 molal. Further, the two indicated distributions for ε_1 are assumed to have a rank correlation of 1.0. Similarly, three triangular distributions with rank correlations of 1.0 are defined for ε_2 for three different sets of conditions. Specifically, each LHS element has two values for ε_1 obtained from the two indicated truncated normal distributions and three values for ε_2 obtained from the three indicated triangular distributions. In addition, the two values for ε_1 have a rank correlation of 1.0 over the entire LHS, and similarly, the three values for ε_2 have a rank correlation of 1.0 over the entire LHS.

As an example, the effect of ε_1 on the release rate of dissolved ^{239}Pu from the EBS as a consequence of an igneous event at 10 yr that destroys all WPs in the repository is illustrated in Fig. 4. Time-dependent release rates of dissolved ^{239}Pu from the EBS (*ESPU239*, g/yr) are shown in Fig. 4a. Each curve in Fig. 3a was generated with one of the 300 LHS elements used in the propagation of epistemic uncertainty in the 2008 YM PA and was calculated with the values for ε_1 and ε_2 in that LHS element.

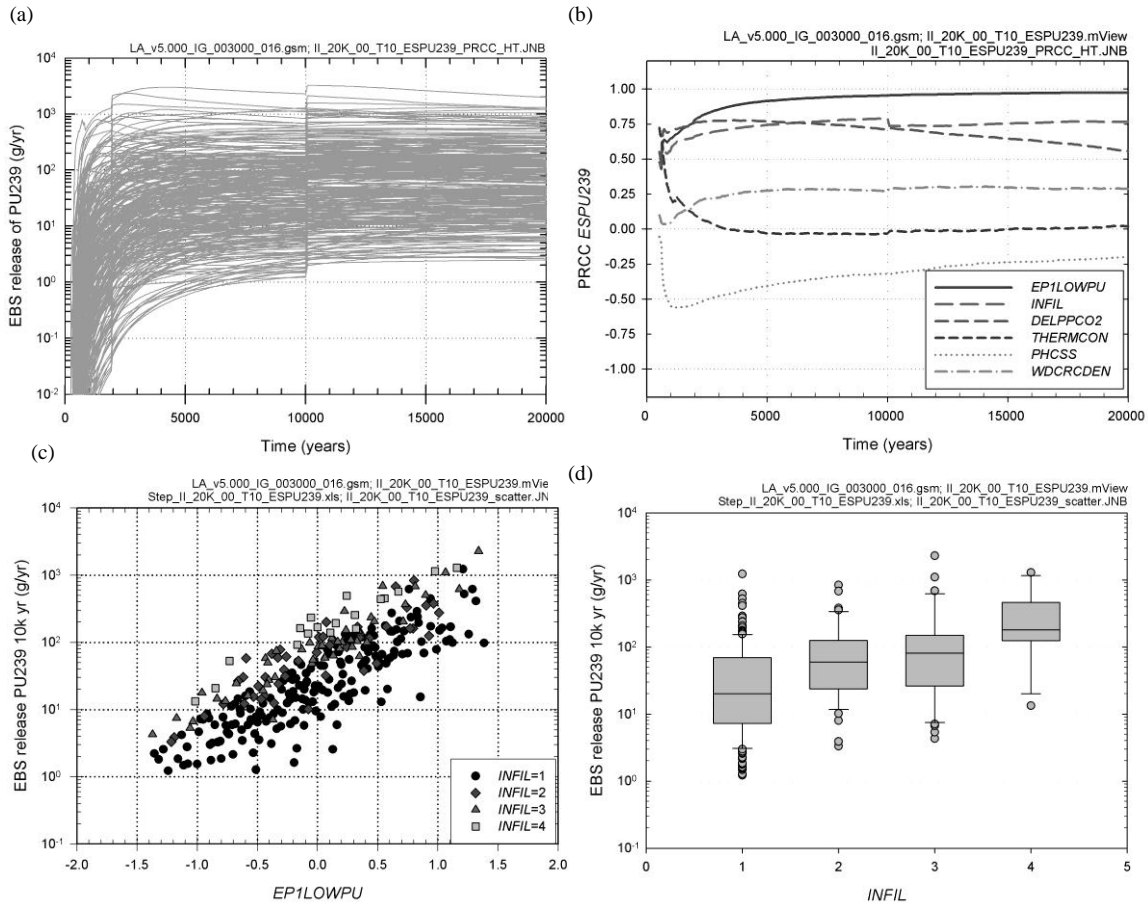


Fig. 4 Release rate of dissolved ^{239}Pu from the EBS ($ESPU_{239}$, g/yr) as a consequence of an igneous event at 10 yr that destroys all WPs in the repository obtained with an LHS of size 300: (a) Time-dependent values for $ESPU_{239}$, (b) Time-dependent partial rank correlation coefficients (PRCCs) for $ESPU_{239}$, (c) scatterplot for $ESPU_{239}$ at 10,000 yr versus $EP1LOWPU$, and (d) Box plots for $ESPU_{239}$ at 10,000 yr conditional on individual values for $INFIL$ ([40], Figs. K6.3.1-7 and K6.3.1-8).

A sensitivity analysis based on partial rank correlation coefficients (PRCCs) is presented in Fig. 4b. Because of the rank correlations associated with the two values for ε_1 and the three values for ε_2 , only one of the two values for ε_1 is included in the analysis, and similarly, only one of the three values for ε_2 is included in the analysis. This is necessary because both regression analyses and partial correlation analyses perform poorly and produce potentially noninformative and/or misleading results when highly correlated predictor variables are present. Only the included value for ε_1 , denoted $EP1LOWPU$ in the 2008 YM PA, was identified as contributing to the epistemic uncertainty associated with $ESPU_{239}$. As shown by the PRCCs in Fig. 4b, $EP1LOWPU$ is the single most important variable affecting the epistemic uncertainty associated with $ESPU_{239}$, with $ESPU_{239}$ tending to increase as $EP1LOWPU$ increases. This effect is not surprising given that the scale factor (i.e., 10^{ε_1}) defined by $EP1LOWPU$ in Eq. (5.2) introduces almost three orders of magnitude of uncertainty into the model for plutonium solubility, which in turn has a similar effect on $ESPU_{239}$.

After *EPILOWPU*, the PRCCs in Fig. 4b indicate smaller effects on *ESPU239* for *DELPPCO2* (scale factor used to incorporate uncertainty into the value for the partial pressure of CO₂), *INFIL* (infiltration level), and *PHCSS* (pointer variable used to determine pH in CSNF cell 1 under liquid influx conditions). The variables *DELPPCO2* and *INFIL* have positive effects on *ESPU239* because (i) increasing *DELPPCO2* increases the partial pressure of CO₂, which, although decreasing pH, also increases the solubility of Pu and thus has a net effect of increasing the amount of dissolved ²³⁹Pu and (ii) increasing *INFIL* increases water flow through the EBS. In contrast, increasing *PHCSS* has a negative effect on *ESPU239* because increasing *PHCSS* increases pH, which (as long as pH is below about 9) tends to decrease Pu solubility.

The PRCCs also indicate effects for *THERMCON* (host rock thermal conductivity level) prior to 1,000 yr. Unfortunately, the effects associated with *THERMCON* result from an implementation error in the version of the model used in these analyses that incorrectly allowed drift-wall condensation to occur after an igneous intrusion ([40], App. P, Table P-6). When condensation occurs, water flow through the waste is increased by the condensation, resulting in the transient spikes in release rates and also in the correlation of release rates and cumulative releases with *THERMCON*. For an igneous intrusion, the indicated cooling occurs but there is no exposed drift wall on which condensation can occur. Further, the variable *WDCRCDEN* (scale factor to convert area on a WP experiencing stress corrosion cracking to a resultant diffusive area) should have no effect on *ESPU239* for igneous intrusive events and thus its selection is most likely spurious as a result of a slight nonrandom pattern in the mapping between the sampled values for *WDCRCDEN* and the calculated values for *ESPU239*.

The dominant effect of *EPILOWPU* on *ESPU239* can be clearly seen in the scatterplot in Fig. 4c. Further, the secondary effect of *INFIL* can be seen in the individually identified points in Fig. 4c and also in the box plots in Fig. 4d. Thus, although the model uncertainty associated with plutonium characterized by *EPILOWPU* dominates the uncertainty in *ESPU239*, the model uncertainty associated with UZ flow properties indexed by *INFIL* also has a significant effect on *ESPU239*.

6. Uncertain Model for Poisson Process

Igneous events are important contributors to expected dose to the RMEI in the 2008 YM PA. In this analysis, the occurrence of igneous events is assumed to follow a Poisson process defined by a rate λ (yr⁻¹). However, significant uncertainty exists with respect to the appropriate value to use for λ in the 2008 YM PA. The nature of λ presents an example of the difficulty of drawing a clear distinction between parameter uncertainty and model uncertainty. From one perspective, a Poisson process is a model defined by the single parameter λ , with the result that uncertainty associated with the appropriate value to use for λ should be viewed as parameter uncertainty. From another perspective, the uncertainty associated with the appropriate value to use for λ derives, at least in part, from uncertainty inherent in the models for igneous processes used in the estimation of λ , with the result that the uncertainty associated with λ can be viewed as having a component that derives from model uncertainty. This is a common situation in many analyses, where the uncertainty associated with a single parameter in one model derives in part from uncertainty in one or more models that underlie the determination of that parameter.

In the 2008 YM PA, λ is (i) represented by the variable *IGRATE*, (ii) assigned a piecewise uniform distribution on the interval $[0, 7.76 \times 10^{-7} \text{ yr}^{-1}]$, and (iii) included in the LHS of size 300 used in the propagation of epistemic uncertainty. The effect of this propagation on expected dose to the RMEI (*EXPDOSE*, mrem/yr) resulting from potential igneous events over 20,000 yr is shown in Fig. 5. Specifically, Fig. 5a shows the 300 time-dependent values for *EXPDOSE* that result from the indicated uncertainty propagation. Each individual curve in Fig. 5a is a plot of the points

$$(\tau, E_A[D_{II}(\tau | \mathbf{a}, \mathbf{e}_M)]), 0 \leq \tau \leq 20,000 \text{ yr}, \quad (6.1)$$

where (i) $D_{II}(\tau | \mathbf{a}, \mathbf{e}_M)$ is the dose to the RMEI (mrem/yr) at time τ (yr) resulting from igneous intrusive events associated with future \mathbf{a} , and (ii) $E_A[D_{II}(\tau | \mathbf{a}, \mathbf{e}_M)]$ corresponds to *EXPDOSE* and is the expected value of $D_{II}(\tau | \mathbf{a}, \mathbf{e}_M)$ over aleatory uncertainty (i.e., over the possible values for \mathbf{a}). Specifically, $E_A[D_{II}(\tau | \mathbf{a}, \mathbf{e}_M)]$ is defined by

$$E_A[D_{II}(\tau | \mathbf{a}, \mathbf{e}_M)] = \int_0^\tau D_{II}(\tau | t, \mathbf{e}_M) \lambda dt, \quad (6.2)$$

where $D_{II}(\tau | t, \mathbf{e}_M)$ is the dose to the RMEI (mrem/yr) at time τ resulting from an igneous intrusive event at time t (yr) (see [40], App. J, for additional discussion). As indicated, $D_{II}(\tau | \mathbf{a}, \mathbf{e}_M)$ and $D_{II}(\tau | t, \mathbf{e}_M)$ are conditional on the values for the epistemically uncertain analysis inputs that constitute the elements of \mathbf{e}_M . Further, λ is an epistemically uncertain input involved in the characterization of aleatory uncertainty and, as a consequence of this role, is an element of the vector \mathbf{e}_A defined in conjunction with Eq. (2.3).

As shown by the PRCCS in Fig. 5b, the uncertainty in *EXPDOSE* is dominated by the uncertainty associated with *IGRATE*, with *EXPDOSE* tending to increase as *IGRATE* increases. This pattern can be seen in the scatterplot in Fig. 5c, where the uncertainty in *EXPDOSE* is clearly dominated by the uncertainty associated with *IGRATE*.

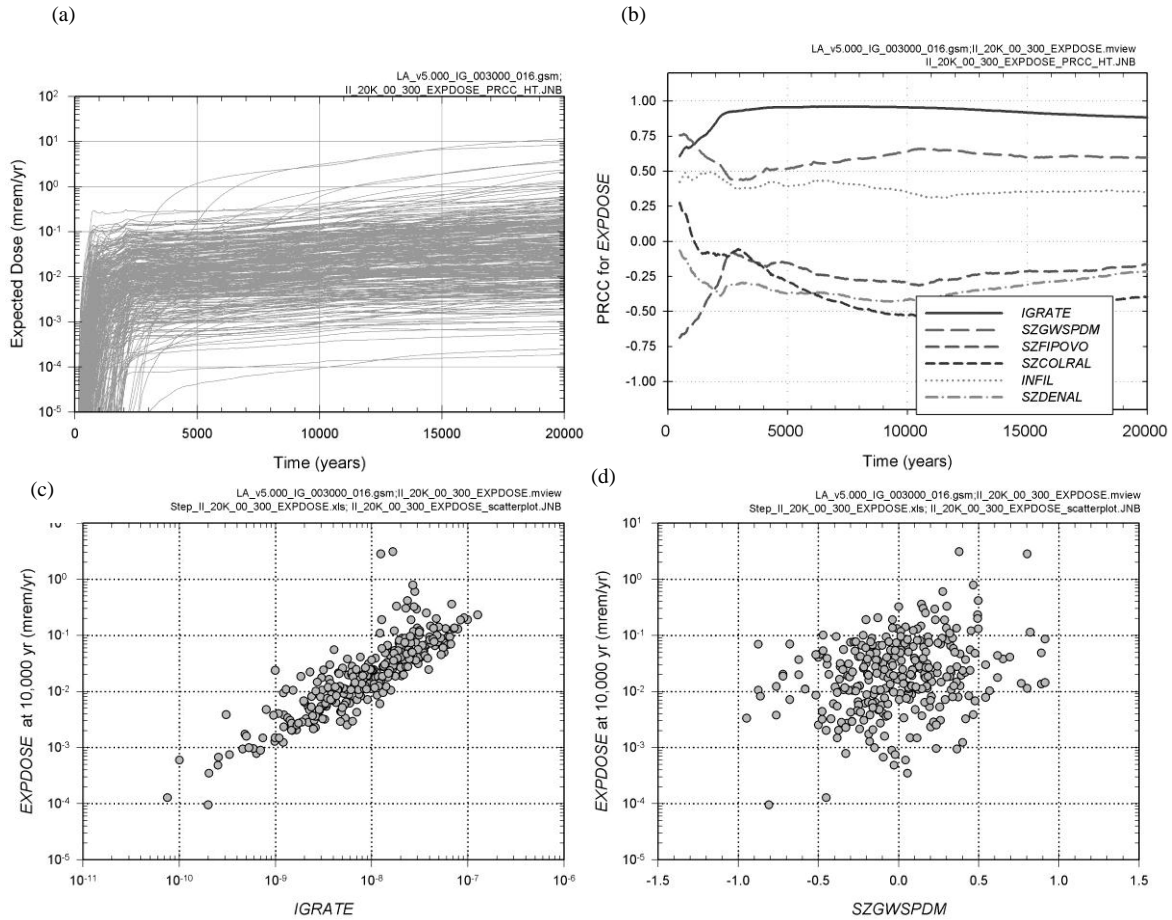


Fig. 5 Expected dose to the RMEI (*EXPDOSE*, mrem/yr) resulting from potential igneous intrusive events obtained with an LHS of size 300: (a) Time-dependent values for *EXPDOSE*, (b) Time-dependent partial rank correlation coefficients (PRCCs) for *EXPDOSE*, (c) scatterplot for *EXPDOSE* at 10,000 yr versus *IGRATE*, and (d) scatterplot for *EXPDOSE* at 10,000 yr versus *SZGWSPDM* ([40], Figs. K6.7.1-1 and K6.7.1-2).

In addition to *IGRATE*, smaller effects are indicated for *SZGWSPDM* (groundwater specific discharge multiplier for the saturated zone (SZ); as sampled, *SZGWSPDM* is actually the logarithm of the indicated multiplier), *SZFIPOVO* (flowing interval porosity in the volcanic unit of the SZ), *SZCOLRAL* (colloid retardation factor in the alluvial unit of the SZ, dimensionless; as sampled, *SZCOLRAL* is actually the logarithm of the indicated retardation factor), *INFIL* (infiltration level), and *SZDENAL* (density of the alluvial unit of the SZ, kg/m^3) (Fig. 5c). The variables *SZGWSPDM* and *INFIL* have positive effects on *EXPDOSE*, with these effects resulting because increasing *SZGWSPDM* increases water flow in the SZ and increasing *INFIL* increases water flow through the EBS and UZ. The variables *SZFIPOVO*, *SZCOLRAL* and *SZDENAL* have negative effects on *EXPDOSE*, with these effects resulting because increasing *SZFIPOVO* slows flow in the SZ and increasing *SZCOLRAL* and *SZDENAL* increases retardation in the alluvial unit of the saturated zone.

For perspective, the scatterplot for *EXPDOSE* versus *SZGWSPDM* is shown in Fig. 5d. The positive effect of *SZGWSPDM* on *EXPDOSE* can be seen in this scatterplot in consistency with the PRCCs for *SZGWSPDM* in Fig. 5b. However, again in consistency with the PRCCs in Fig.

5b, comparison of the scatterplots for *IGRATE* and *SZGWSPDM* clearly shows the dominant effect of *IGRATE* on the uncertainty in *EXPDOSE*.

As discussed at the beginning of this section, uncertainty in λ could be viewed as either parameter uncertainty or model uncertainty. One step up in complexity involves an analysis that must incorporate a hazard curve rather than a simple stationary Poisson process as in the example of this section. As used here, a hazard curve corresponds to a function that defines the annual frequencies at which an occurrence of interest produces an effect that exceeds a given size. For example, $\lambda_i(N)$ could be a hazard curve where $\lambda_i(N)$ is the annual frequency (yr^{-1}) at which igneous events occur at the YM repository that damage $N + 1$ or more WPs; as another example, $\lambda_s(v)$ could be a hazard curve where $\lambda_s(v)$ is the annual frequency (yr^{-1}) at which seismic events occur at a given nuclear power plant that have peak ground velocities that exceed v . Uncertainty in the appropriate definition of a hazard curve can be appropriately viewed as model uncertainty as hazard curves arise from a combination of data and modeling.

7. Uncertain Model for Dose Conversion

The appropriate consideration of the uncertainty inherent in the calculation of potential environmental radiation exposures was an important part of the 2008 YM PA. Core components of this calculation are dose conversion factors that convert environmental radionuclide concentrations (e.g., Bq/L) to dose to the RMEI (e.g., mrem/yr) [55]. The consideration of over 20 radionuclides and several different environmental conditions resulted in a large number of dose conversion factors for incorporation into the 2008 YM PA. Further, extensive correlations exist between the individual dose conversion factors as a result of the use of the same uncertain quantities in the calculation of many different dose conversion factors. When considered in the large, the dose conversion model can be viewed as a complex model that produces a vector of dose conversion factors. Because of the many uncertainties involved in the calculation of dose conversion factors, significant uncertainties and correlations are present in the dose conversion factors produced by this model. Because of their overall complexity, these uncertainties and correlations can be collectively viewed as a form of model uncertainty.

The incorporation of the uncertainty in the dose conversion factors into the determination of dose to the RMEI was a major challenge in the 2008 YM PA. The development of a complex correlation structure involving the dose conversion factors and the incorporation of this correlation structure into the LHS used in the propagation of epistemic uncertainty was not practicable as a consequence of the large number of dose conversion factors involved. Instead, the strategy described in the next paragraph was employed.

A separate uncertainty analysis using an LHS of size 1000 was carried out for the dose conversion model. This analysis sampled $nU = 309$ uncertain quantities used in the determination of dose conversion factors ([55], Table 6.6-2). For each LHS element, the dose conversion model calculated the resultant vector of dose conversion factors. The result was 1000 vectors of dose conversion factors. Further, the appropriate correlation structure exists across these vectors of dose conversion factors because the dose conversion factors in each vector were calculated with the same set of values for uncertain quantities used as input to the dose conversion model. The result of this analysis was then incorporated into the final analysis for the 2008 YM PA through the use of a pointer variable that had a uniform distribution on the integers 1, 2, ..., 1000, where

each integer designates one of the 1000 previously generated vectors of dose conversion factors. Specifically, each element of the final LHS of size 300 had one sampled value for this pointer variable, and the corresponding vector of dose conversion factors was then used in all dose calculations for that LHS element. With this approach, the uncertainty and appropriate correlation structure for the dose conversion factors was incorporated into the 2008 YM PA without having to include all the dose conversion factors in the generation of the final LHS used in the 2008 YM PA and also without having to deduce the complex correlation structure associated with the dose conversion factors and then incorporate this correlation structure in the final LHS.

As an example, results for dose to the RMEI from ^{99}Tc (*DOTC99*, mrem/yr) resulting from an igneous intrusion at 10 yr that destroys all WPs in the repository are shown in Fig. 6. Specifically, Fig. 6a shows the 300 time-dependent values for *DOTC99* that result from the indicated uncertainty propagation. Because no solubility limit or chemical retardation is assumed for ^{99}Tc in the 2008 YM PA and the igneous event under consideration is assumed to destroy all WPs in the repository, the repository's ^{99}Tc inventory is quickly released from the EBS and transported to the location of the RMEI. This behavior can be seen in Fig. 6a in the rapid peaking in *DOTC99* at about 1000 yr followed by a steady decrease in *DOTC99* after this peak.

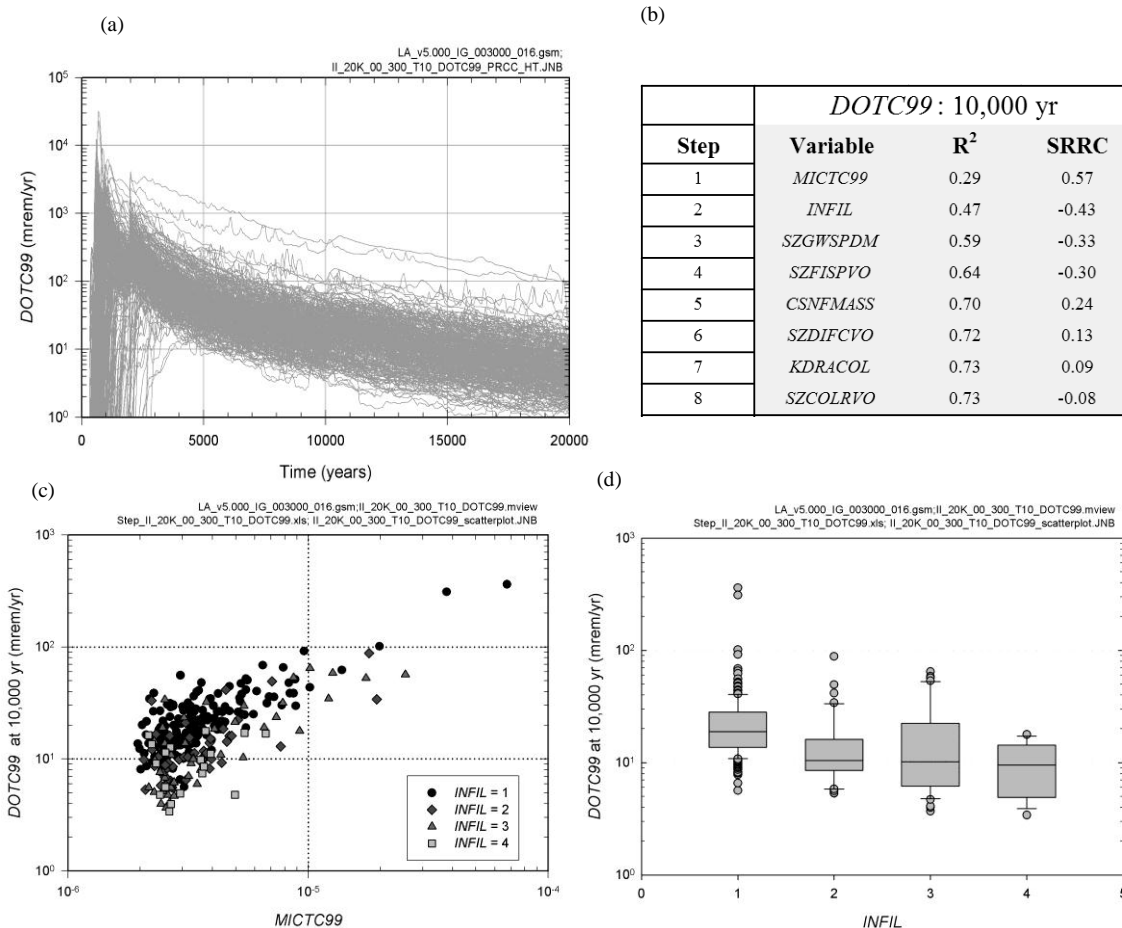


Fig. 6: Dose to the RMEI from ^{99}Tc ($DOTC99$, mrem/yr) resulting from an igneous intrusion at 10 yr that destroys all WPs in the repository obtained with an LHS of size 300: (a) Time-dependent values for $DOTC99$, (b) stepwise rank regression for $DOTC99$ at 10,000 yr, (c) scatterplot for $DOTC99$ at 10,000 yr versus $MICTC99$, and (d) Box plots for $DOTC99$ at 10,000 yr conditional on individual values for $INFIL$ ([40], Figs. K6.6.1-9 and K6.6.1-10).

A sensitivity analysis for $DOTC99$ at 10,000 yr based on stepwise rank regression is presented in Fig. 6b (see discussion associated with Fig. 2c for a description of stepwise rank regression). The first variable picked in the analysis is the dose conversion factor $MICTC99$ (dose conversion factor for ^{99}Tc for modern interglacial climate, (rem/yr)/(pCi/L)), with $DOTC99$ tending to increase with increasing values for $MICTC99$ as indicated by the the positive SRRC. This effect can also be seen in the scatterplot in Fig. 6c. After $MICTC99$, three variables having negative effects on $DOTC99$ are selected: $INFIL$ (infiltration level), $SZGWSPDM$ (groundwater specific discharge multiplier for the SZ; as sampled, $SZGWSPDM$ is actually the logarithm of the indicated multiplier), and $SZFI SPVO$ (flowing interval spacing in the volcanic unit of the SZ, m). The negative effects associated with these variables results because increasing their values increases the early release of ^{99}Tc (i.e, in the vicinity of 500 - 1000 yr; see Fig. 6a) and thus results in less ^{99}Tc at the location of the RMEI at 10,000 yr. As an example, the effect of $INFIL$ can be seen in the scatterplot in Fig. 6d, with $DOTC99$ decreasing with increasing values for $INFIL$. This effect results because increasing $INFIL$ increases water flow through the

EBS, which in turn increases early removal of ^{99}Tc from the EBS and thus results in less ^{99}Tc being present at later times to result in dose to the RMEI. After *INFIL*, *SZGWSPDM* and *SZFISPVO*, small positive effects are indicated for *CSNFMASS* (scale factor used to characterize uncertainty in amount of CSNF in CSNF WPs) and *SZDIFCVO* (logarithm of effective diffusion coefficient in fractured volcanic units, m^2/s), with the positive effect of *CSNFMASS* resulting from its role in defining the amount of ^{99}Tc in the repository and the positive effect of *SZDIFCVO* resulting from its role in slowing the transport of ^{99}Tc in the saturated zone. The selection of *KDRACOL* (distribution coefficient for reversible sorption of radium onto uranophane colloids, mL/g) at the end of the regression is spurious.

8. Summary Discussion

As indicated by the five presented examples, there is no clear dividing line between parameter uncertainty and model uncertainty. Rather, there is a gradation from situations that correspond more closely to the concept of model uncertainty as the existence of different possibly appropriate conceptual structures to represent a complex process (e.g., the examples in Sects. 3-5) to situations that correspond more closely to the concept of parameter uncertainty as the lack of knowledge with respect to the appropriate value to use for a single real-valued quantity that is an input to a model (e.g., the examples in Sects. 6-7). Complicating the distinction between model uncertainty and parameter uncertainty is that most single real-valued quantities used as input to a model for a complex process (e.g., a spatially averaged permeability used as input to a model for radionuclide transport in flowing ground water) are actually summaries in the uncertainty of what would be the outcome of a very complex modeling process if all the factors that gave rise to the single value under consideration were taken into account. As a consequence, many ostensible parameter uncertainties are, at least in part, summaries of the implications of model uncertainty.

Model uncertainty should be thought of in terms of appropriateness for a particular analysis. No model for a complex process is correct in the sense of having complete fidelity with respect to all aspects of the process under consideration. As a result, no model is fully correct. Thus, when probability is used to characterize model uncertainty, the question being asked should be with respect to appropriateness for use in a particular analysis rather than with respect to correctness in some absolute sense.

Verification and validation are important components in the assessment of model uncertainty, where (i) verification is the process of determining that a model implementation accurately represents the developers' conceptual description of the model and the solution to the model, and (ii) validation is the process of determining the degree to which a model is an accurate representation of the real world from the perspective of the intended uses of the model (p. 3, [56]; [5; 6; 57-60]). Verification is important to reducing, and hopefully eliminating, the part of model uncertainty that derives from concerns with respect to the correctness of the computational implementation of a model. Further, model validation is an important contributor to the insights that ultimately lead to a characterization of model uncertainty.

As a consequence of the diverse sources of information that will often underlie the quantification of model uncertainty in a particular analysis, it is likely that such quantification will involve some form of expert review process [61-72]. For such review, it is very important that the reviewers understand the details of the particular analysis under consideration so that their assessments of model uncertainty are with respect to the appropriateness of the potential models for that analysis.

In developing probability distributions to characterize model uncertainty, the goal should be to develop distributions that provide an unbiased characterization of the uncertainty with respect to the appropriate model to use in the analysis under consideration. In particular, such distributions should provide uncertainty characterizations that are neither deliberately pessimistic (i.e., conservative) nor deliberately optimistic (i.e., nonconservative). The importance of avoiding conservative analyses has been emphasized by a number of individuals, including a chairman of the NRC [73-77]. Ideally, if deliberate conservatism is to be included in an analysis, this conservatism should be incorporated after a nonconservative analysis has been performed. With this approach, the shifting of the results of the analysis by the addition of one or more conservative assumptions can be clearly identified and understood. For example, such an analysis could be of benefit in making a convincing argument for the safety of the system under consideration. However, without first carrying out an unbiased analysis, there is no way to meaningfully assess the effects, and hence the potential benefits and detriments, of skewing analysis results through the imposition of conservative assumptions. As an example, this approach underlies the compliance certification for the Waste Isolation Pilot Plant (WIPP), where an initial PA was carried out by the DOE [78; 79] and then a modification of this PA was carried out with changes specifically requested by the EPA [80].

Probability is the mathematical structure that has traditionally been used to represent model uncertainty. However, other mathematical structures exist that could potentially be used to represent model uncertainty (e.g., interval analysis, fuzzy set theory, possibility theory, evidence theory) [81-91]. It is possible that some of these other structures for the representation of uncertainty might be of use in characterizing model uncertainty. In particular, evidence theory is appealing because it provides a way to distinguish between the amount of information that supports a proposition and the absence of information that refutes a proposition

Acknowledgments

Work performed at Sandia National Laboratories (SNL), which is a multiprogram laboratory operated by Sandia Corporation, a Lockheed Martin Company, for the U.S. Department of Energy's (DOE's) National Nuclear Security Administration under Contract No. DE-AC04-94AL85000. The views expressed in this article are those of the authors and do not necessarily reflect the views or policies of the DOE or SNL. The United States Government retains and the publisher, by accepting this article for publication, acknowledges that the United States Government retains a non-exclusive, paid-up, irrevocable, world-wide license to publish or reproduce the published form of this article, or allow others to do so, for United States Government purposes.

9. References

1. Christie MA, Glimm J, Grove JW, Higdon DM, Sharp DH, Wood-Schultz MM. Error Analysis and Simulations of Complex Phenomena. *Los Alamos Science* 2005;29:6-25.
2. Saltelli A, Ratto M, Tarantola S, Campolongo F. Sensitivity Analysis for Chemical Models. *Chemical Reviews* 2005;105(7):2811-2828.
3. Wagner RL. Science, Uncertainty and Risk: The Problem of Complex Phenomena. *APS News* 2003;12(1):8.
4. Oberkampf WL, DeLand SM, Rutherford BM, Diegert KV, Alvin KF. Error and Uncertainty in Modeling and Simulation. *Reliability Engineering and System Safety* 2002;75(3):333-357.
5. Oberkampf WL, Trucano TG. Verification and Validation in Computational Fluid Dynamics. *Progress in Aerospace Sciences* 2002;38(3):209-272.
6. Trucano TG, Swiler LP, Igusa T, Oberkampf WL, Pilch M. Calibration, Validation, and Sensitivity Analysis: What's What. *Reliability Engineering and System Safety* 2006;91(10-11):1331-1357.
7. Blower SM, Dowlatabadi H. Sensitivity and Uncertainty Analysis of Complex Models of Disease Transmission: an HIV Model, as an Example. *International Statistical Review* 1994;62(2):229-243.
8. Breeding RJ, Helton JC, Gorham ED, Harper FT. Summary Description of the Methods Used in the Probabilistic Risk Assessments for NUREG-1150. *Nuclear Engineering and Design* 1992;135(1):1-27.
9. Helton JC. Uncertainty and Sensitivity Analysis in the Presence of Stochastic and Subjective Uncertainty. *Journal of Statistical Computation and Simulation* 1997;57(1-4):3-76.
10. Helton JC, Burmaster DE. Guest Editorial: Treatment of Aleatory and Epistemic Uncertainty in Performance Assessments for Complex Systems. *Reliability Engineering and System Safety* 1996;54(2-3):91-94.
11. Helton JC. Treatment of Uncertainty in Performance Assessments for Complex Systems. *Risk Analysis* 1994;14(4):483-511.
12. Paté-Cornell ME. Uncertainties in Risk Analysis: Six Levels of Treatment. *Reliability Engineering and System Safety* 1996;54(2-3):95-111.
13. Parry GW. The Characterization of Uncertainty in Probabilistic Risk Assessments of Complex Systems. *Reliability Engineering and System Safety* 1996;54(2-3):119-126.
14. Parry GW, Winter PW. Characterization and Evaluation of Uncertainty in Probabilistic Risk Analysis. *Nuclear Safety* 1981;22(1):28-42.
15. Apostolakis G. The Concept of Probability in Safety Assessments of Technological Systems. *Science* 1990;250(4986):1359-1364.
16. Iman RL, Helton JC. An Investigation of Uncertainty and Sensitivity Analysis Techniques for Computer Models. *Risk Analysis* 1988;8(1):71-90.
17. Iman RL, Helton JC, Campbell JE. An Approach to Sensitivity Analysis of Computer Models, Part 1. Introduction, Input Variable Selection and Preliminary Variable Assessment. *Journal of Quality Technology* 1981;13(3):174-183.

18. Iman RL, Helton JC, Campbell JE. An Approach to Sensitivity Analysis of Computer Models, Part 2. Ranking of Input Variables, Response Surface Validation, Distribution Effect and Technique Synopsis. *Journal of Quality Technology* 1981;13(4):232-240.
19. Iman RL, Conover WJ. Small Sample Sensitivity Analysis Techniques for Computer Models, with an Application to Risk Assessment. *Communications in Statistics: Theory and Methods* 1980;A9(17):1749-1842.
20. Helton JC. Uncertainty and Sensitivity Analysis Techniques for Use in Performance Assessment for Radioactive Waste Disposal. *Reliability Engineering and System Safety* 1993;42(2-3):327-367.
21. Hamby DM. A Review of Techniques for Parameter Sensitivity Analysis of Environmental Models. *Environmental Monitoring and Assessment* 1994;32(2):135-154.
22. Saltelli A, Chan K, E.M. Scott (eds). *Sensitivity Analysis*. New York, NY: Wiley, 2000.
23. Frey HC, Patil SR. Identification and Review of Sensitivity Analysis Methods. *Risk Analysis* 2002;22(3):553-578.
24. Helton JC, Johnson JD, Sallaberry CJ, Storlie CB. Survey of Sampling-Based Methods for Uncertainty and Sensitivity Analysis. *Reliability Engineering and System Safety* 2006;91(10-11):1175-1209.
25. Helton JC, Davis FJ. Illustration of Sampling-Based Methods for Uncertainty and Sensitivity Analysis. *Risk Analysis* 2002;22(3):591-622.
26. Drogue EL, Mosleh A. Bayesian methodology for model uncertainty using model performance data. *Risk Analysis* 2008;28(5):1457-1476.
27. Brock WA, Durlauf SN, West KD. Model uncertainty and policy evaluation: Some theory and empirics. *Journal of Econometrics* 2007;136(2):629-664.
28. Refsgaard JC, van der Sluijs JP, Brown J, van der Keur P. A framework for dealing with uncertainty due to model structure error. *Advances in Water Resources* 2006;29(11):1586-1597.
29. Beven K. A manifesto for the equifinality thesis. *Journal of Hydrology* 2006;320(1-2):18-36.
30. Beven K. Towards a coherent philosophy for modelling the environment. *Proceedings of the Royal Society A: Mathematical, Physical and Engineering Sciences* 2002;458(2026):2465-2484.
31. Laskey KB. Model Uncertainty: Theory and Practical Implications. *IEEE Transactions on Systems, Man, and Cybernetics--Part A: Systems and Humans* 1996;26(3):340-348.
32. Zio E, Apostolakis GE. Two methods for the structured assessment of model uncertainty by experts in performance assessments of radioactive waste repositories. *Reliability Engineering and System Safety* 1996;54(2-3):225-241.
33. Draper D. Assessment and Propagation of Model Uncertainty. *Journal of the Royal Statistical Society, Series B* 1995;57(1):45-97.
34. Mosleh A, Siu N, Smidts C, Liu C. *Proceedings of Workshop I in Advanced Topics in Risk and Reliability Analysis, Model Uncertainty: Its Characterization and Quantification*. NUREG/CP-0138. Washington, D.C.: U.S. Nuclear Regulatory Commission 1994.
35. U.S. DOE (U.S. Department of Energy). *Final Environmental Impact Statement for a Geologic Repository for the Disposal of Spent Nuclear Fuel and High-Level Radioactive Waste at Yucca Mountain, Nye County, Nevada*. DOE/EIS-0250F. Washington, D.C.: U.S. Department of Energy, Office of Civilian Radioactive Waste Management 2002.

36. U.S. DOE (U.S. Department of Energy). *Yucca Mountain Science and Engineering Report, Rev. 1*. DOE/RW-05391. Washington, D.C.: U.S. Department of Energy, Office of Civilian Radioactive Waste Management 2002.
37. CRWMS M&O (Civilian Radioactive Waste Management System Management and Operating Contractor). *Total System Performance Assessment for the Site Recommendation*. TDR-WIS-PA-000001 REV 00. Las Vegas, NV: CRWMS M&O 2000.
38. U.S. DOE (U.S. Department of Energy). *Viability Assessment of a Repository at Yucca Mountain*. DOE/RW-0508. Washington, D.C.: U.S. Department of Energy, Office of Civilian Radioactive Waste Management 1998.
39. USGS (U.S. Geological Survey). *Yucca Mountain as a Radioactive Waste Repository*. Circular 1184. Denver, CO: USGS Information Services 1999.
40. SNL (Sandia National Laboratories). *Total System Performance Assessment Model/Analysis for the License Application*. MDL-WIS-PA-000005 Rev 00, AD 01. Las Vegas, NV: U.S. Department of Energy Office of Civilian Radioactive Waste Management 2008.
41. Helton JC, Hansen CW, Sallaberry CJ. Yucca Mountain 2008 Performance Assessment: Conceptual Structure and Computational Implementation. In. *Proceedings of the International High-Level Radioactive Waste Management Conference, September 7-11, 2008*: American Nuclear Society, 2008:524-532.
42. U.S. NRC (U.S. Nuclear Regulatory Commission). 10 CFR Part 63: Implementation of a Dose Standard after 10,000 Years. *Federal Register* 2009;74(48):10811-10830.
43. U.S. NRC (U.S. Nuclear Regulatory Commission). 10 CFR Part 63: Implementation of a Dose Standard after 10,000 Years. *Federal Register* 2005;70(173):53313-53320.
44. U.S. NRC (U.S. Nuclear Regulatory Commission). 10 CFR Parts 2, 19, 20, etc.: Disposal of High-Level Radioactive Wastes in a Proposed Geologic Repository at Yucca Mountain, Nevada; Final Rule. *Federal Register* 2001;66(213):55732-55816.
45. Helton JC, Sallaberry CJ. Conceptual Basis for the Definition and Calculation of Expected Dose in Performance Assessments for the Proposed High-Level Radioactive Waste Repository at Yucca Mountain, Nevada. *Reliability Engineering and System Safety* 2009;94:677-698.
46. Helton JC. Mathematical and Numerical Approaches in Performance Assessment for Radioactive Waste Disposal: Dealing with Uncertainty. In: EM Scott, ed. *Modelling Radioactivity in the Environment*. New York, NY: Elsevier Science, 2003:353-390.
47. Feller W. *An Introduction to Probability Theory and Its Applications*, Vol. 2, 2nd edn. New York, NY: John Wiley & Sons, 1971.
48. McKay MD, Beckman RJ, Conover WJ. A Comparison of Three Methods for Selecting Values of Input Variables in the Analysis of Output from a Computer Code. *Technometrics* 1979;21(2):239-245.
49. Helton JC, Davis FJ. Latin Hypercube Sampling and the Propagation of Uncertainty in Analyses of Complex Systems. *Reliability Engineering and System Safety* 2003;81(1):23-69.
50. BSC (Bechtel SAIC Company). *Future Climate Analysis*. ANL-NBS-GS-000008 REV 01. Las Vegas, NV: Bechtel SAIC Company 2004.
51. SNL (Sandia National Laboratories). *Data Analysis for Infiltration Modeling: Extracted Weather Station Data Used to Represent Present-Day and Potential Future Climate Conditions in the Vicinity of Yucca Mountain*. ANL-MGR-MD-000015 REV 00. Las Vegas, NV: Sandia National Laboratories 2006.

52. SNL (Sandia National Laboratories). *Simulation of Net Infiltration for Present-Day and Potential Future Climates*.MDL-NBS-HS-000023 REV 01 AD 01.Las Vegas, NV: Sandia National Laboratories 2007.
53. SNL (Sandia National Laboratories). *UZ Flow Models and Submodels*.MDL-NBS-HS-000006 REV 03 AD 01.Las Vegas, NV: Sandia National Laboratories 2007.
54. SNL (Sandia National Laboratories). *Engineered Barrier System: Physical and Chemical Environment*.ANL-EBS-MD-000033 REV 06.Las Vegas, NV: Sandia National Laboratories 2007.
55. SNL (Sandia National Laboratories). *Biosphere Model Report*.MDL-MGR-MD-000001 REV 02.Las Vegas, Nevada: Sandia National Laboratories 2007.
56. American Institute of Aeronautics and Astronautics. *AIAA Guide for the Verification and Validation of Computational Fluid Dynamics Simulations*.AIAA G-077-1998.Reston, VA: American Institute of Aeronautics and Astronautics 1998.
57. Roache PJ. *Verification and Validation in Computational Science and Engineering*. Albuquerque, NM: Hermosa Publishers, 1998.
58. Oberkampf WL, Trucano TG, Hirsch C. Verification, Validation, and Predictive Capability in Computational Engineering and Physics. *Applied Mechanics Review* 2004;57(5):345-384.
59. Roache PJ. Building PDE Codes to be Verifiable and Validatable. *Computing in Science & Engineering* 2004;6(5):30-38.
60. Babuska I, Oden JT. Verification and Validation in Computational Engineering and Science: Basic Concepts. *Computer Methods in Applied Mechanics and Engineering* 2004;193(36-38):4057-4066.
61. Garthwaite PH, Kadane JB, O'Hagan A. Statistical Methods for Eliciting Probability Distributions. *Journal of the American Statistical Association* 2005;100(470):680-700.
62. Cooke RM, Goossens LHJ. Expert Judgement Elicitation for Risk Assessment of Critical Infrastructures. *Journal of Risk Research* 2004;7(6):643-656.
63. Ayyub BM. *Elicitation of Expert Opinions for Uncertainty and Risks*.Boca Raton, FL: CRC Press 2001.
64. McKay M, Meyer M. Critique of and Limitations on the Use of Expert Judgements in Accident Consequence Uncertainty Analysis. *Radiation Protection Dosimetry* 2000;90(3):325-330.
65. Budnitz RJ, Apostolakis G, Boore DM, Cluff LS, Coppersmith KJ, Cornell CA, Morris PA. Use of Technical Expert Panels: Applications to Probabilistic Seismic Hazard Analysis. *Risk Analysis* 1998;18(4):463-469.
66. Evans JS, Gray GM, Sielken Jr. RL, Smith AE, Valdez-Flores C, Graham JD. Use of Probabilistic Expert Judgement in Uncertainty Analysis of Carcinogenic Potency. *Regulatory Toxicology and Pharmacology* 1994;20(1, pt. 1):15-36.
67. Chhibber S, Apostolakis G, Okrent D. A Taxonomy of Issues Related to the Use of Expert Judgments in Probabilistic Safety Studies. *Reliability Engineering and System Safety* 1992;38(1-2):27-45.
68. Thorne MC, Williams MMR. A Review of Expert Judgement Techniques with Reference to Nuclear Safety. *Progress in Nuclear Safety* 1992;27(2-3):83-254.
69. Cooke RM. *Experts in Uncertainty: Opinion and Subjective Probability in Science*. Oxford; New York: Oxford University Press, 1991.

70. Keeney RL, Winterfeldt DV. Eliciting Probabilities from Experts in Complex Technical Problems. *IEEE Transactions on Engineering Management* 1991;38(3):191-201.
71. Meyer MA, Booker JM. *Eliciting and Analyzing Expert Judgment: A Practical Guide*. New York, NY: Academic Press, 1991.
72. Hora SC, Iman RL. Expert Opinion in Risk Analysis: The NUREG-1150 Methodology. *Nuclear Science and Engineering* 1989;102(4):323-331.
73. Diaz NJ. Realism and Conservatism, Remarks by Chairman Diaz at the 2003 Nuclear Safety Research Conference, October 20, 2003. In. *NRC News*. No. S-03-023. Washington, D.C.: U.S. Nuclear Regulatory Commission., 2003.
74. Paté-Cornell E. Risk and Uncertainty Analysis in Government Safety Decisions. *Risk Analysis* 2002;22(3):633-646.
75. Caruso MA, Cheok MC, Cunningham MA, Holahan GM, King TL, Parry GW, Ramey-Smith AM, Rubin MP, Thadani AC. An Approach for Using Risk Assessment in Risk-Informed Decisions on Plant-Specific Changes to the Licensing Basis. *Reliability Engineering and System Safety* 1999;63:231-242.
76. Sielken RL, Jr., Bretzlaff RS, Stevenson DE. Challenges to Default Assumptions Stimulate Comprehensive Realism as a New Tier in Quantitative Cancer Risk Assessment. *Regulatory Toxicology and Pharmacology* 1995;21:270-280.
77. Nichols AL, Zeckhauser RJ. The Perils of Prudence: How Conservative Risk Assessments Distort Regulation. *Regulatory Toxicology and Pharmacology* 1988;8:61-75.
78. U.S. DOE (U.S. Department of Energy). *Title 40 CFR Part 191 Compliance Certification Application for the Waste Isolation Pilot Plant*. DOE/CAO-1996-2184, Vols. I-XXI. Carlsbad, NM: U.S. Department of Energy, Carlsbad Area Office, Waste Isolation Pilot Plant 1996.
79. Helton JC, Marietta MG. Special Issue: The 1996 Performance Assessment for the Waste Isolation Pilot Plant. *Reliability Engineering and System Safety* 2000;69(1-3):1-451.
80. MacKinnon RJ, Freeze G, Jow H-N. *Summary of EPA-Mandated Performance Assessment Verification Test (Replicate 1) and Comparison with the Compliance Certification Application Calculations*. Technical Data Package (Sandia WIPP Central Files WPO #46674). Albuquerque, NM: Sandia National Laboratories 1997.
81. Helton JC, Johnson JD, Oberkampf WL, Sallaberry CJ. Representation of Analysis Results Involving Aleatory and Epistemic Uncertainty. *International Journal of General Systems To appear*.
82. Klir GJ. *Uncertainty and Information: Foundations of Generalized Information Theory*. Hoboken, NJ: Wiley, 2005.
83. Helton JC, Johnson JD, Oberkampf WL. An Exploration of Alternative Approaches to the Representation of Uncertainty in Model Predictions. *Reliability Engineering and System Safety* 2004;85(1-3):39-71.
84. Klir GJ. Generalized Information Theory: Aims, Results, and Open Problems. *Reliability Engineering and System Safety* 2004;85(1-3):21-38.
85. Ross TJ. *Fuzzy Logic with Engineering Applications*, 2nd edn. New York, NY: Wiley, 2004.
86. Halpern JY. *Reasoning about Uncertainty*. Cambridge, MA: MIT Press, 2003.
87. Ross TJ, Booker JM, W.J. Parkinson (eds.). *Fuzzy Logic and Probability Applications: Bridging the Gap*. Philadelphia, PA: Society for Industrial and Applied Mathematics, 2002.

88. Jaulin L, Kieffer M, Didrit O, Walter E. *Applied Interval Analysis*. New York, NY: Springer-Verlag, 2001.
89. Wolkenhauer O. *Data Engineering: Fuzzy Mathematics in Systems Theory and Data Analysis*. New York, NY: Wiley, 2001.
90. Klir GJ, Wierman MJ. *Uncertainty-Based Information*. New York, NY: Physica-Verlag 1999.
91. Yager RR, Kacprzyk J, M. Fedrizzi (eds). *Advances in the Dempster-Shafer Theory of Evidence*. New York, NY: Wiley, 1994.